# Membrane-less hybrid flow battery based on low-cost elements

P.K. Leung[1,2], T. Martin[1], A.A. Shah[3,*] , M.R. Mohamed[4], M.A. Anderson[1], J. Palma[1]

1. IMDEA Energy, Mostoles, Madrid, 28935, Spain.

2. Department of Materials, University of Oxford, Oxford, OX1 3PH, UK.

3. School of Engineering, University of Warwick, Coventry, CV4 7AL, UK.

4. Faculty of Electrical & Electronics, Universiti Malaysis Pahang, 26600, Malaysia.

## Abstract

The capital cost of conventional redox flow batteries is relatively high (> USD$ 200 /kWh) due to the use of expensive active materials and ion-exchange membranes. This paper presents a membrane-less hybrid organic-inorganic flow battery based on the low-cost elements zinc (< USD$ 3 $Kg^{-1}$) and para-benzoquinone (< USD$ 8 $Kg^{-1}$). Redox potential and voltammetric studies show that the open-circuit voltage of the battery is 1.17 – 1.59 V over a wide range of pH. Half-cell charge-discharge and dissolution experiments indicate that the negative electrode reaction is limiting due to the presence of chemical side reactions on the electrode surface. The positive electrode redox reactions are not affected and exhibit (half-cell) coulombic efficiencies of > 92.7 % with the use of carbon felt electrodes. In the presence of a fully oxidized active species close to its solubility limit, dissolution of the deposited anode is relatively slow (< 2.37 g $h^{-1}$ $cm^{-2}$) with an equivalent corrosion current density of < 1.9 mA $cm^{-2}$. In a parallel plate flow configuration, the resulting battery was charge-discharge cycled at 30 mA $cm^{-2}$ with average coulombic and energy efficiencies of *c.a.* 71.8 and *c.a.* 42.0 % over 20 cycles, respectively.

***Keywords:*** Flow battery; para-benzoquinone; hybrid; low cost; membrane-less.

## Introduction

Ambitious targets for cutting greenhouse gas emissions [1] are reliant on the wide-scale deployment of intermittent renewable energy technologies (notably solar and wind) on a grid-scale [2]. To enable the use of such technologies, in particular to provide a stable energy output to end-users, competitive energy storage systems are required to balance load with demand [3–6]. To ensure that energy storage systems are economically competitive in the long term, the US Department of Energy (DoE) has set a long-term capital cost target of USD$ 150/kWh to match the costs of existing physical energy storage technologies [7].

Redox flow batteries have emerged as the most promising energy storage system in terms of cost and safety for applications of a few kW/kWh up to tens of MW/MWh. The main advantage of this technology over conventional rechargeable batteries is the ability to decouple capacity from power effectively by adjusting the electrode size and/or the electrolyte volume [5]. The shelf life of redox flow batteries is theoretically long since most cell components (i.e. plastic

*Corresponding author. *Tel*: +44 (0)2476 151676. *Fax*: +44 (0)2476 418922. *Email*: Akeel.Shah@warwick.ac.uk

and carbon) do not corrode or deteriorate over time, considering that the active redox species can be separated once the battery is charged.

Since the invention of the redox flow battery, various chemistries have been proposed (e.g., all-vanadium [8], zinc-cerium [9] and vanadium-cerium [10]) and most use expensive ion-exchange membranes to separate the negative and positive electrolytes. At the present time, the all-vanadium redox flow battery is the most developed system, due to its high reversibility and large power output, as well as the fact that the redox species remain in solution at all times. However, the capital cost of this system (> USD$ 200/kWh) exceeds the proposed DoE target for extensive market penetration. The current cost of vanadium is around USD$ 23 – 25 $Kg^{-1}$, which represents around 30 % of the overall capital cost of the battery. The costs of the ion-exchange membranes and electrodes are estimated to be *c.a.* 41 % in the cost model illustrated in Figure 1, consistent with existing literature [11].

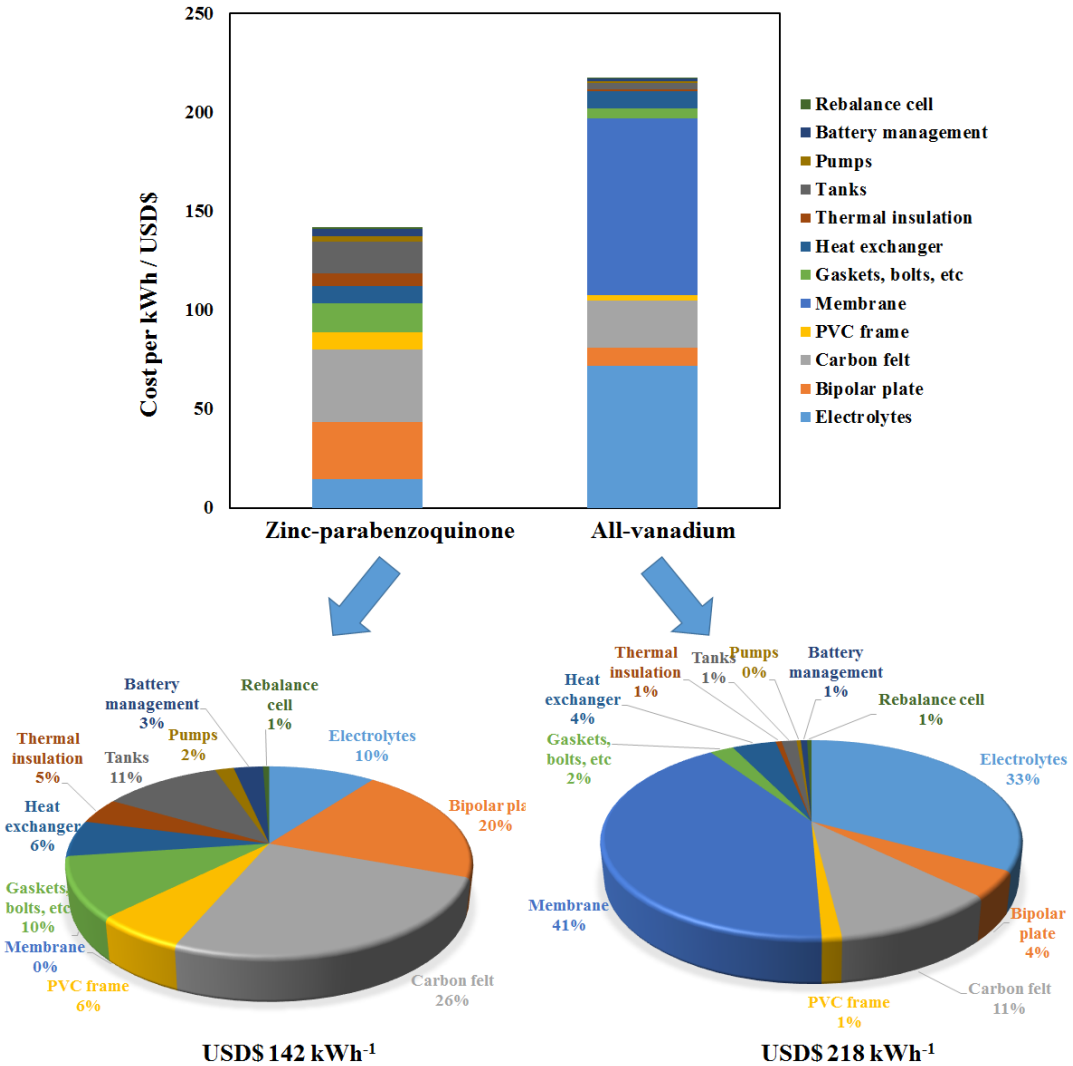


***Figure 1*** Capital cost breakdown of 1MW × 10 h redox flow batteries: (a) comparison between zinc-benzoquinone (pBQ) and all-vanadium chemistries. Detailed descriptions and calculations are available in Supplementary Information. Component costs are based on Ref. [12].

Aiming to reduce costs and simplify the cell design, several membrane-less systems have been proposed, including the soluble lead acid [13 – 14], zinc-nickel [15 – 16], copper-lead dioxide [17], cadmium-chloranil [18], zinc-lead dioxide [19 – 20] and zinc-cerium [21 – 22] redox flow batteries. Some of these proposed systems make use of the slow dissolution processes of deposited metals in the presence of certain active species in the electrolytes. For certain chemistries, the capacities of the batteries are still limited by the positive electrode reactions, particularly those relying on a solid-phase transformation within the electrode materials (e.g., chloro-benzoquinone/chloro-hydroquinone [18], $PbO_2/PbSO_4$ [13 – 14], $NiOOH/Ni(OH)_2$ [15 – 16]). In order to address these issues, it is preferable to use soluble active species rather than species undergoing a solid-phase transformation for both of the electrode reactions and should exhibit low corrosion rates at the anode. The chemistry should be based on low-cost active materials (< USD$ 10 $Kg^{-1}$) and should lead to a voltage of > 1.0 V.

In order to achieve the low costs required, several studies have investigated the use of abundant organic active materials based on common elements, such as carbon, hydrogen, oxygen and sulfur [23, 24]. These organic molecules can be tailored to have certain properties, such as fast kinetics, high solubility and high associated cell voltage in the resulting flow battery [25-28]. They typically dissolve in either aqueous or non-aqueous electrolytes and can be incorporated in polymers [29] or appear as solid electrodes mixed with porous carbon and binders [30].

Aqueous based chemistries are considered in this work since the ionic conductivity of water is significantly higher ($6 \times 10^{-8}$ S $cm^{-1}$ [31]) than that of pure organic solvents ($1 \times 10^{-8}$ S $cm^{-1}$ for propylene carbonate, $6 \times 10^{-10}$ S $cm^{-1}$ for propylene carbonate [31]). Furthermore, the costs of non-aqueous solvents (e.g.. USD$ 1.5 – 1.7 per $dm^3$ for propylene carbonate [32]) are up to one hundred times higher than of water (< USD$ 0.004 per $dm^3$) [33] for industrial applications.

In an attempt to increase the cell voltage and/or specific energy further, inorganic redox couples can be combined with organic species in hybrid organic-inorganic systems, as reported recently in several studies (anthraquinone-bromide [23], alloxazine-ferricyanide [34] and anthraquinone-ferricyanide [35]). Despite relatively high cell voltages (0.86 V – 1.2 V), the inorganic redox couples involved are either toxic or hazardous [23, 34, 35].

In this work, we propose for the first time the use of zinc (< USD$ 3 $Kg^{-1}$) and para-benzoquinone (< USD$ 8 $Kg^{-1}$) as the redox couples in a hybrid organic-inorganic flow battery, which is, moreover, membrane-less. Among the various organic materials, quinone is used as the active material due to its high chemical stability (benzene ring) and reversibility for flow battery applications [36]. Faciliated by previous computational screening [37], benzoquinone compounds as the parent isomers were reported to have higher solubilities (*c.a.* 100 mM) and to lead to more positive electrode potentials than naphthoquinone and anthraquinone.

Parabenzoquinone (pBQ) is the prototypical member the quinone family. Its chemistry and reaction products are well understood. In most cases, organic molecules can be oxidized or reduced to a number of reaction products, including radicals. According to the Pourbaix diagram [38], the possible reaction products at certain pH values (e.g., pH 7) can only be parabenzoquinone (pBQ) and hydroquinone (HQ). The side reactions can only be the decompositions of water (hydrogen and oxygen evolution).

Due to the low-cost of these active materials, the electrolyte cost is expected to be less than USD$ 15/kWh, leading to an overall capital cost of < USD $ 150/kWh (see Figure 1 and Supplementary Information). In the typical charge-discharge process, the negative electrode reactions are the electrodeposition and dissolution of zinc on a planar substrate material:

$$Zn^{2+} + 2\,e^- \leftrightarrow Zn \qquad E_0 = -0.76 \text{ V } vs. \text{ SHE} \quad (1)$$

At the positive electrode, the primary reaction is the oxidation of hydroquinone (HQ) and the reduction of para-benzoquinone (pBQ) during charge and discharge, respectively:

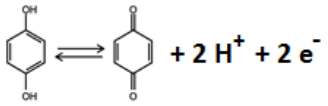


$E_0 = +0.64$ V *vs.* SHE (2)

The proposed electrode reactions have been proven to be highly reversible with the use of carbon-based electrodes and they involve two-electron transfers, resulting in a high specific capacity. Since a separator is not required in this configuration, a single electrolyte is circulated through the battery for both the negative and positive electrode reactions. The operating concept is based on the efficiency of the reactions and the slow rate of dissolution at the anode. The use of carbon felt electrodes facilitates the redox reactions of the organic active species at the positive electrode. Furthermore, the presence of the quinone molecule does not necessarily hinder the electrodeposition process, since hydroquinone (HQ) is also used as an electrolyte additive in metal plating [39].

The main challenge of this system is the self-discharge process caused by the dissolution of zinc in the presence of the oxidized active species. This process can be controlled by using low concentrations of the hydroquinone (HQ)/benzoquinone (pBQ) species, considering that the solubility of the oxidized species is *c.a.* 100 mmol $dm^{-3}$ in aqueous solutions. By evaluating the influences of the aforementioned issues, this work provides a preliminary proof-of-concept of the first membrane-less organic-inorganic flow battery based on low-cost elements. Experimental results show that the resulting system has an open-circuit voltage of > 1.1 V and is capable of charge-discharge cycling at an average energy efficiency of *c.a.* 44.1 % over 20 cycles.

## 2. Experimental details

### 2.1. Chemicals

Analytical grade zinc chloride, 1,4-benzoquinone (also known as parabenzoquinone, pBQ), 1,4-hydroquinone (HQ), sodium hydroxide and reagent grade aqueous hydrochloric acid were supplied from Sigma Aldrich (Germany) and Fisher Scientific (UK). Solutions were prepared with ultra-pure water (18 MΩ cm resistivity) from a Millipore water purification system (Milli-Q Integral 3). A metallic zinc sample of 1.6 mm thickness (foil, code: 10438, 99 % purity) was supplied by Alfa Aesar (UK). Typical starting electrolytes for flow battery testing contained 1.5 mol $dm^{-3}$ zinc chloride and 50 mmol $dm^{-3}$ hydroquinone (HQ). Unless specified, the electrolyte pH values were usually between 6 and 7 without using hydrochloric acid or sodium hydroxide solutions.

### 2.2. Cyclic voltammetry

Cyclic voltammetry was conducted in a conventional three-electrode glass cell with approximately 20 $cm^3$ electrolyte volume. A glassy carbon electrode with an exposed area of 0.07 $cm^2$ was used as the working electrode. Counter and reference electrodes were platinum and silver-silver chloride (Ag|AgCl, 1 mol $dm^{-3}$ KCl, ABB, Series 1400, Switzerland). The cyclic voltammetry measurements were made using a Bio-logic VMP potentiostat (Bio-logic SAS, France) for both the negative zinc and positive quinone reactions in an electrolyte containing 10 mmol $dm^{-3}$ active materials (zinc(II) chloride and hydroquinone (HQ)) in 1.0 mol $dm^{-3}$ sodium chloride. To evaluate the effect of pH on the electrochemical behaviour of the two reactions, electrolytes were adjusted between pH 1 and 12 using sodium hydroxide or hydrochloric acid solutions. For the zinc electrodeposition reaction, cyclic voltammetry was carried out between the potential ranges of –0.5 and –1.6 V *vs.* Ag|AgCl at a potential sweep rate of 80 mV $s^{-1}$. Similarly, cyclic voltammetry was carried out between –0.3 and +1.2 V *vs.* Ag|AgCl at the same potential sweep rate (80 mV $s^{-1}$) for the positive electrode reaction.

### 2.3. Zinc dissolution tests

Measurements of the zinc dissolution rate were carried out in different electrolyte compositions, similarly to methods reported elsewhere [40]. To ensure that the surface conditions of different samples were identical, zinc samples were supplied from Alfa Aesar (1.6 mm thickness, 99 %, Ref. 10438, United Kingdom). The dimensions of these samples were *c.a.* 9.5 mm × *c.a.* 9.0 mm × *c.a.* 1.6 mm and their surfaces were pretreated by manually polishing with silicon carbide paper grade P120, degreasing with detergent, and etching in concentrated acid (30 % HCl, 30 % $H_2SO_4$) for 30 s to obtain a light, matte, clean surface. Following these procedures, the samples were ultrasonic cleaned for 1 minute and rinsed with ultrapure water (Milli-Q Integral 3). The total exposed areas of the zinc sample surfaces were in the range 2.3 – 2.5 $cm^2$. The zinc samples were removed and weighed every few hours using an electronic balance (± 0.01 g accuracy, Scout Pro SP202, Ohaus, United States). After each measurement, the zinc samples were returned to the electrolytes. The experimental procedures described above were repeated over a total period of 168 – 190 hours. The zinc dissolution rate can be represented by corrosion current density, $j_{cor}$, which can be measured from the average gravimetric values based on the weight loss measurements [40, 41]. To ensure that the concentration of the parabenzoquinone (pBQ) is relatively constant over time, solution volumes of 100 – 300 $cm^3$ were used. From Faraday's law of electrolysis, the average rate of weight loss at a constant current density $j_{cor}$ is given by:

$$\mathrm{d}w/\mathrm{d}t = M\, j_{cor}\, A \,/\, z\, F \tag{3}$$

where $M$ is the molar mass of zinc (g $mol^{-1}$), $A$ is the area exposed to the electrolyte ($m^2$), $z$ is the number of electrons transferred and $F$ is the Faraday constant (C $mol^{-1}$).

### 2.4. Flow battery experiments

The charge-discharge performance of the electrode reactions was evaluated in a commercial flow battery (Proingesa, Spain) based on a membrane-less configuration, similar to that in previous work [42]. Figure 2 shows the experimental arrangement and electrolyte circuits of the

proposed system. The single cell consisted of two electrodes, two acrylic flow channels (2 mm thickness each) and four neoprene rubber gaskets (1 mm thickness each). There was one inlet at the lower side of the positive electrode and one outlet at the upper side of the negative electrode. The reference electrode was silver-silver chloride (0.1 mol $dm^{-3}$ KOH, equipped with a liquid junction protection tube, ABB, Switzerland) placed at the entrance of the inlet, in line with the electrolyte circuit.

The overall electrolyte and electrical circuits are presented in Figure 2 [21 – 22]. Within the flow battery, planar carbon polyvinylester (2.0 cm × 2.0 cm, Electrocell, Denmark) was used as the substrate material for both the negative and positive electrodes. In the case of the positive electrode, a piece of carbon felt (2.0 cm × 2.0 cm, Sigratherm GFA-05, SGL Carbon, 5 mm thickness, Germany) was attached on the substrate material with the use of polyester tapes (Cole-Parmer Inc., United States). Unless otherwise indicated, a single electrolyte of 1.5 mol $dm^{-3}$ zinc chloride and 50 mmol $dm^{-3}$ hydroquinone (HQ) (volume 40 $cm^3$) adjusted to pH 7 was circulated through the battery at a volumetric flow rate of *c.a.* 90 $cm^3$ $min^{-1}$.

In order to ensure an efficient zinc electrodeposition process, the negative planar carbon electrode was charge-discharge cycled at 30 mA $cm^{-2}$ in a pure 1.5 mol $dm^{-3}$ zinc(II) chloride solution to obtain more than 90 % half-cell coulombic efficiencies over 20 cycles. In typical charge-discharge experiments, negative and positive currents (40 – 320 mA; 10 – 80 mA $cm^{-2}$) were applied at the working electrodes for a specified period of time, engendering the reduction and the oxidation processes. The current densities are always referred to the negative two-dimensional electrode (2.0 cm × 2.0 cm) due to the higher surface areas of the positive electrodes. To evaluate the influence of the electrolyte compositions on each half-cell reaction, the working electrode potentials of the two electrodes were measured independently. In the case of full-cell experiments, the cell voltage was estimated by subtracting the negative from the positive potential. The cut-off voltage was set at 0.8 V during the discharge process. All electrochemical measurements were made using a Bio-logic VMP potentiostat (Bio-logic SAS, France). The negative and positive electrode potentials and overall cell voltages were continuously monitored.

The coulombic, voltage and energy efficiencies of the redox flow battery were calculated from the following formulae:

$$\text{Coulombic efficiency} = j_d \Delta t_d / j_c \Delta t_c \text{ x } 100\ \% \quad (4)$$

$$\text{Voltage efficiency} = V_d / V_c \text{x } 100\ \% \quad (5)$$

$$\text{Energy efficiency} = j_d V_d \Delta t_d / j_c V_c \Delta t_c \text{ x } 100\ \% \quad (6)$$

where $V$ is the cell voltage, $j$ is the applied current density, $\Delta t_c$ is the charge duration and $\Delta t_d$ is the discharge duration; subscripts $c$ and $d$ denote the charge and discharge processes, respectively.

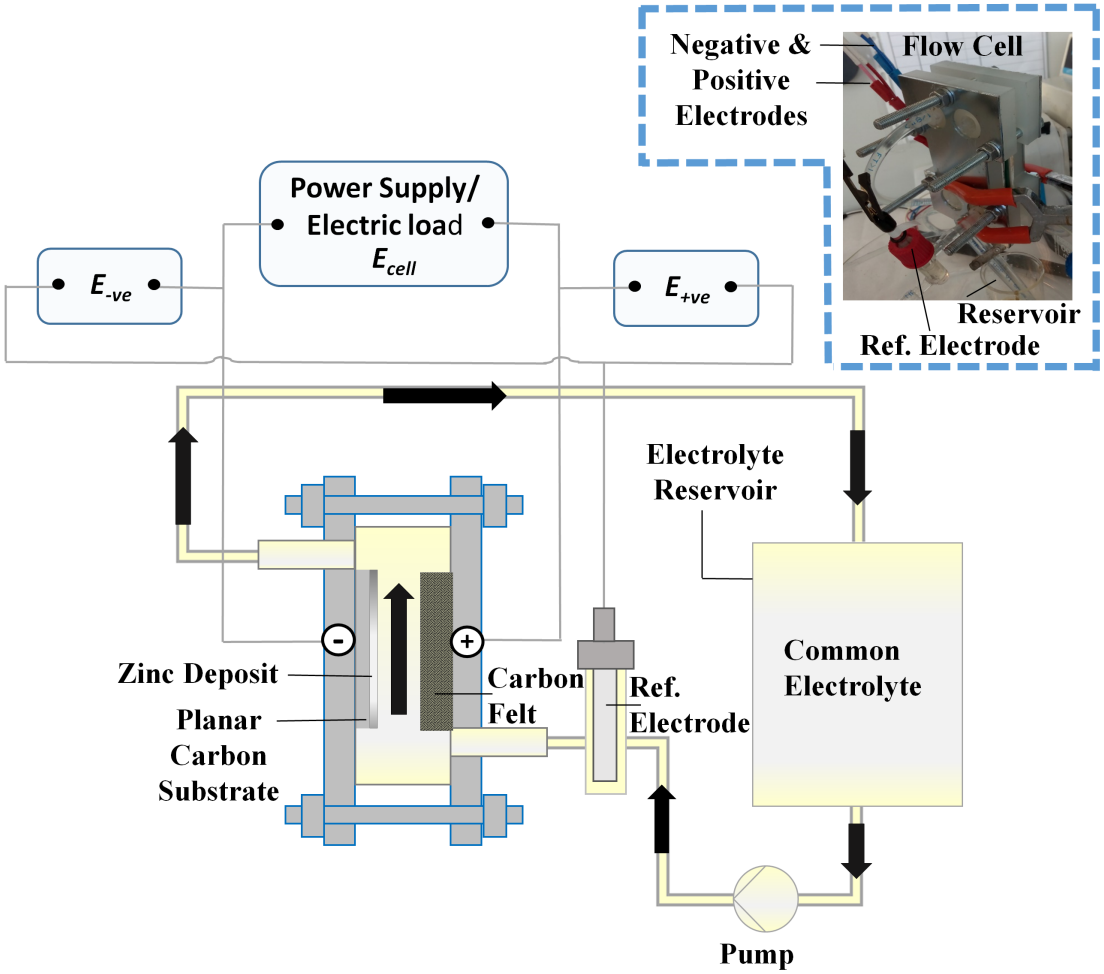


***Figure 2*** Schematic of the experimental arrangement and the electrolyte circuits for the proposed membrane-less zinc-benzoquinone (BQ) flow battery.

## 3. Results and discussion

### 3.1. Redox potentials

For the development of this battery chemistry, it is important to identify the possible cell voltage range for typical operations. Estimates of the cell voltages can be obtained by measuring the half-cell potentials. In this study, the half-cell potentials were measured at open-circuit in the presence of the charged products (i.e. 100 % state of charge (SOC)). For instance, the formal potentials of the negative and positive electrodes were measured by cyclic voltammetry using metallic zinc and glassy carbon electrodes, respectively, in the electrolyte containing 10 mmol $dm^{-3}$ zinc or parabenzoquinone (pBQ) in 1 mol $dm^{-3}$ sodium chloride solution (pH adjusted using hydrochloric acid or sodium hydroxide). Figure 3 shows the recorded potentials of both the negative and positive electrodes at open-circuit conditions under a wide range of pH values. It can be seen that the cell voltages were higher than 1.17 V and dependent on the pH of the solution.

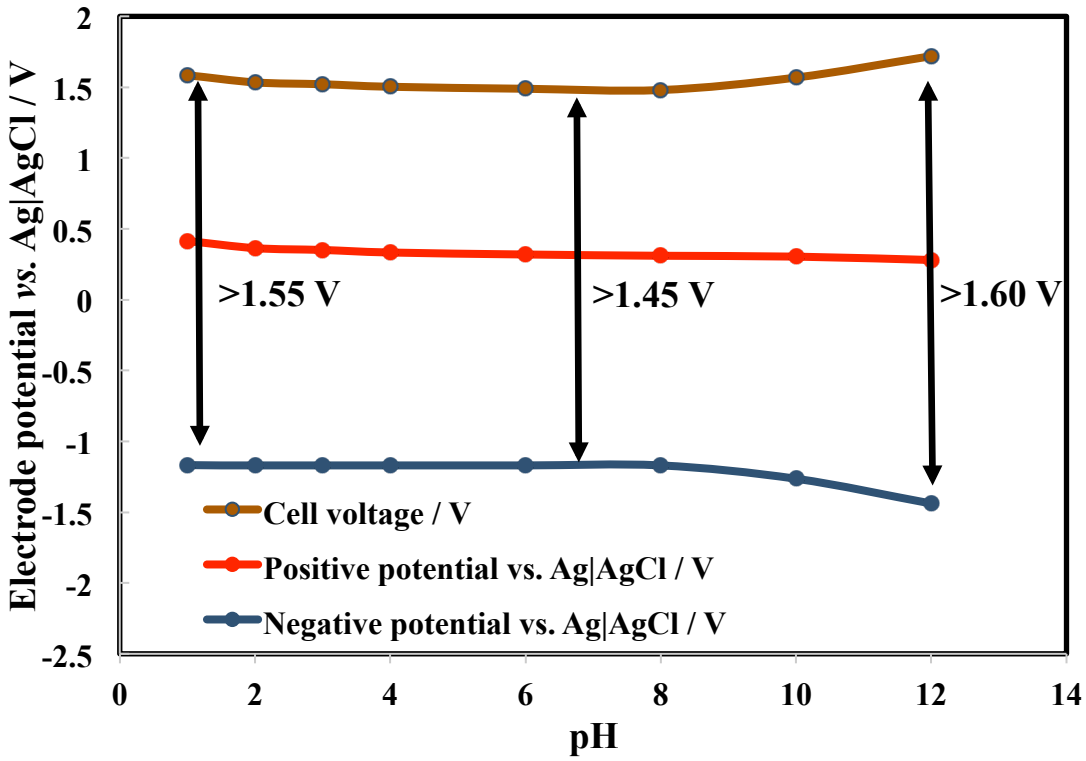


***Figure 3*** Open-circuit potentials *vs.* pH of the zinc, parabenzoquinone (pBQ) electrode potentials as well as the overall cell in 1 mol $dm^{-3}$ sodium chloride solution (adjusted by hydrochloric acid or sodium hydroxide).

As shown in Figure 3, a two-proton-two-electron gradient (– 59 mV $pH^{-1}$) was observed for the parabenzoquinone (pBQ) reaction (reaction (2)) between pH 1 and 3 (between 1 and 2 protons are involved at pH 3 – 12 as the gradients were > – 59 mV $pH^{-1}$), while a zero-proton gradient (0 mV $pH^{-1}$) was observed for the zinc reaction (reaction (1)) between pH 1 and 8. The overall cell voltage was higher with increased acidity and alkalinity, up to > 1.55 V (*c.a.* pH 1 and 12). The increase in cell voltage in more acidic and alkaine solutions can be attributed to the redox potentials of the parabenzoquinone (pBQ) and zinc reactions, respectively. As reported elsewhere, the reduction of parabenzoquinone (pBQ) in alkaline solutions could lead to several products, such as semi-quinone ($Q^{-}$), quinone dianion ($Q^{2-}$) and the protonated anion ($QH^{-}$), which are less chemically stable compared to hydroquinone ($QH_2$ or HQ) obtained in acidic solutions [43]. The precise proportions of these compounds depend on the p$K_a$ values and the total concentration of the quinone species. On the contrary, the possible reaction products in neutral electrolytes (i.e. pH 7) can only be parabenzoquinone (pBQ) and hydroquinone (HQ). For these reasons, the battery chemistry is considered to be more suitable for operation in such electrolyte conditions (pH 7).

### 3.2. Electrochemical behaviour

The electrochemical behaviour of the negative zinc and the positive parabenzoquinone (pBQ) half-cells was characterized using cyclic voltammetry. Figure 4 shows the combined cyclic

voltammograms of the zinc (left) and parabenzoquinone (pBQ) (right) half-cell reactions at pH 1 and 7, in which the measurements for each half-cell reaction were made individually. The voltammetry of zinc electrodeposition was carried out by sweeping the potentials linearly from –0.5 to –1.6V *vs.* Ag|AgCl at 80 mV $s^{-1}$, while that of parabenzoquinone (pBQ) reduction was recorded by scanning between –0.3 and +1.2 V *vs.* Ag|AgCl at the same potential sweep rate. A relatively low concentration of 10 mmol $dm^{-3}$ was used for both active species to avoid significant ohmic drops at increased current densities.

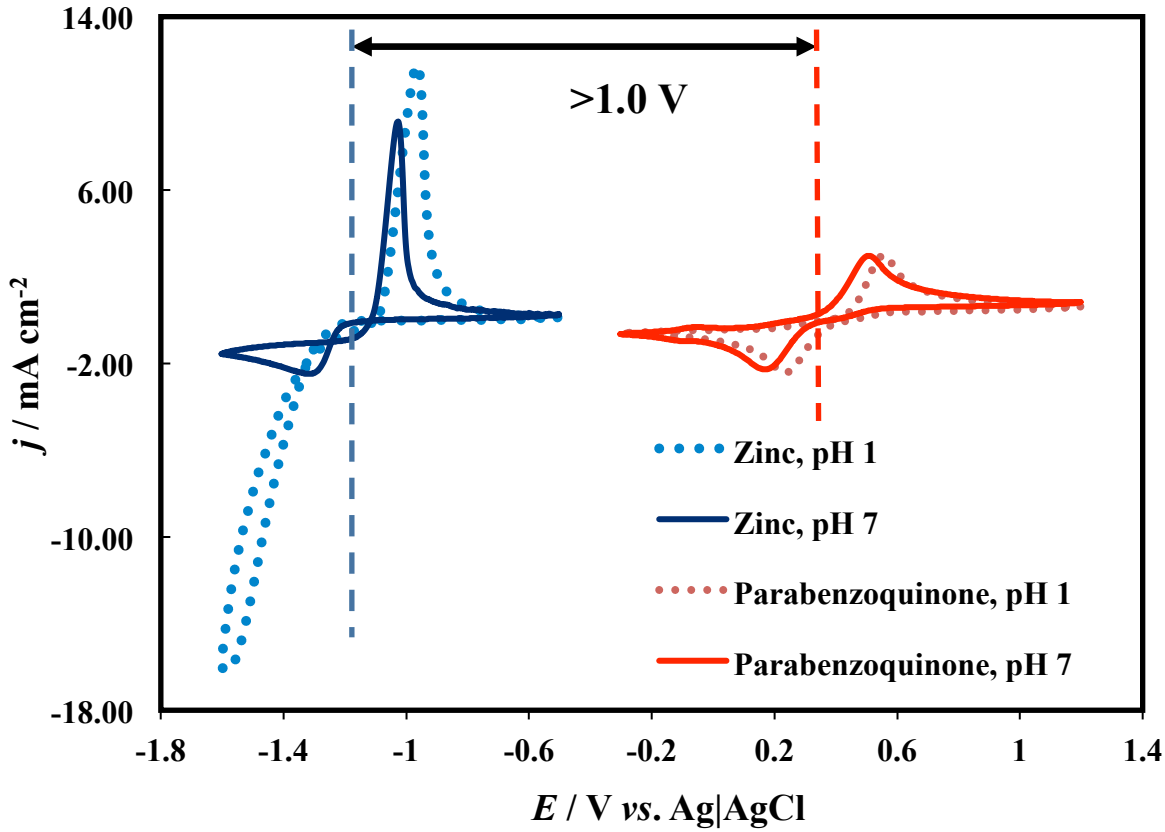


***Figure 4*** Combined cyclic voltammograms of the zinc and parabenzoquinone (pBQ) electrodes in 1 mol $dm^{-3}$ sodium chloride solution (adjusted by hydrochloric acid or sodium hydroxide). Potential sweep rate: 80 mV $s^{-1}$; electrolytes: 10 mmol $dm^{-3}$ $ZnCl_2$ or hydroquinone (HQ) in 1 mol $dm^{-3}$ sodium chloride solutions; substrate: glassy carbon electrode; room temperature. HQ is the reduced species, pBQ is the oxidized species.

The cyclic voltammograms of the two reactions are similar to those reported elsewhere. During charge, zinc electrodeposition in the negative half-cell takes place with the oxidation of hydroquinone (HQ) at the positive electrode. In the cyclic voltammogram, zinc electrodeposition becomes appreciable at approximately –1.2 V *vs.* Ag|AgCl and forms a cathodic peak at – 1.35 V *vs.* Ag|AgCl. Since the standard electrode potential of zinc (–0.76 V *vs.* SHE) is more negative than that of hydrogen evolution (0 *vs.* SHE), hydrogen evolution could take place as a side reaction at pH 1, as indicated by a sharp increase in the cathodic current densities at more negative electrode potentials (< –1.35 V *vs.* SHE). Hydrogen evolution

leads to a very low coulombic efficiency (less than 30 %). On the other hand, the redox reactions of hydroquinone (HQ)/benzoquinone (pBQ) are initiated at an electrode potential of +0.4 V *vs.* Ag|AgCl at pH 7. Based on the $E_0$ *vs.* pH plot, the electrode potential tends to shift towards more positive values in acidic media with a similar peak separation (*c.a.* 317 – 330 mV). Taking into account the side reaction, an acidic solution with a pH lower than 7 is not suitable for a reversible battery system.

### 3.3. Electrolyte formulations

Due to the membrane-less configuration, a common electrolyte was used for both the negative and positive half-cell reactions. Since the common electrolyte contains the active speicies for both electrode reactions, optimized electrolyte compositions are important to ensure high system efficiencies (coulombic and voltage). In contrast to the voltammetric studies, concentrated zinc(II) chloride (1.5 mol $dm^{-3}$) was used to avoid mass transport limitations and to act as conductive salt. As reported elsewhere, the use of concentrated solutions (e.g. 1.5 mol $dm^{-3}$) can minimize the dissolution of zinc in aqueous electrolytes [40]. In this work, 50 mmol $dm^{-3}$ hydroquinone (HQ) was added in the common electrolyte as the initial species for the positive electrode reaction. The use of such a low concentration was motivated by the solubility limit of the oxidized benzoquinone species (*c.a.* 100 mmol $dm^{-3}$) in pure water. For measurements related to the zinc and parabenzoquinone (pBQ) reactions, the working electrodes were carbon-polyvinyl ester substrates and carbon felt, respectively, while the counter electrodes were either metallic zinc or platinized titanium.

#### 3.3.1. Influence of hydrochloric acid

Based on the half-cell potential measurements, the influence of the hydrochloric acid concentration on the evolutions of the electrode potentials for both reactions is illustrated in Figures 5a and 5b. Each half-cell was charge-discharge cycled individually using a three-electrode set-up at a constant current density of 30 mA $cm^{-2}$ (120 mA). The use of this current density is restricted by the planar deposited anode, as in most hybrid flow batteries. The applied current densities used in conventional zinc-bromine batteries are usually < 30 mA $cm^{-2}$ [44, 45].

Both the charge and discharge phases were 15 min in duration. The charge capacity was equivalent to an overall SOC of *c.a.* 55 % based on the energy content of the parabenzoquinone species (pBQ). Since the half-cell measurements were independent, we were able to identify the limiting reaction of the resulting battery. In the absence of acid (0 mol $dm^{-3}$ HCl, pH 7), the average charge potentials for the negative and positive electrode reactions were *c.a.* –1.06 V and *c.a.* +0.35 V *vs.* Ag|AgCl, respectively, while the average values for discharge were *c.a.* –0.89 V and +0.04 V *vs.* Ag|AgCl, respectively. The coulombic efficiencies of both reactions were more than 86 %. This indicates that both redox species were well utilized at the end of the discharge phase. Since the coulombic efficiencies of the negative zinc half-cell reactions (*c.a.* 86 %) were lower than those of the positive quinone reaction (*c.a.* 92 %), the negative zinc reaction was limiting.

With the addition of hydrochloric acid, the half-cell coulombic efficiency of the zinc reaction decreased significantly from *c.a.* 86 % to *c.a.* 78 % at 1.0 mold $dm^{-3}$ and to *c.a.* 67 % at 2.0 mol

$dm^{-3}$. This is attributed to a less efficient zinc electrodeposition associated with the evolution of hydrogen during charge, as well as the direct reaction of zinc with protons when it is no longer cathodically protected during the discharge process. In comparison, the half-cell coulombic efficiencies of the parabenzoquinone (pBQ) reaction were stable (*c.a.* 92 %), while the potential difference between the charge and discharge profiles decreased slightly at higher acid concentrations (310 mV at 0 mol $dm^{-3}$ HCl *vs.* 220 mV at 2.0 mol $dm^{-3}$ HCl), which is consistent with the voltammetric findings discussed in Section 3.2. Taking into account the side reactions, a less acidic or neutral electrolyte, such as a pH 7 electrolyte, is more suitable for the proposed membrane-less battery.

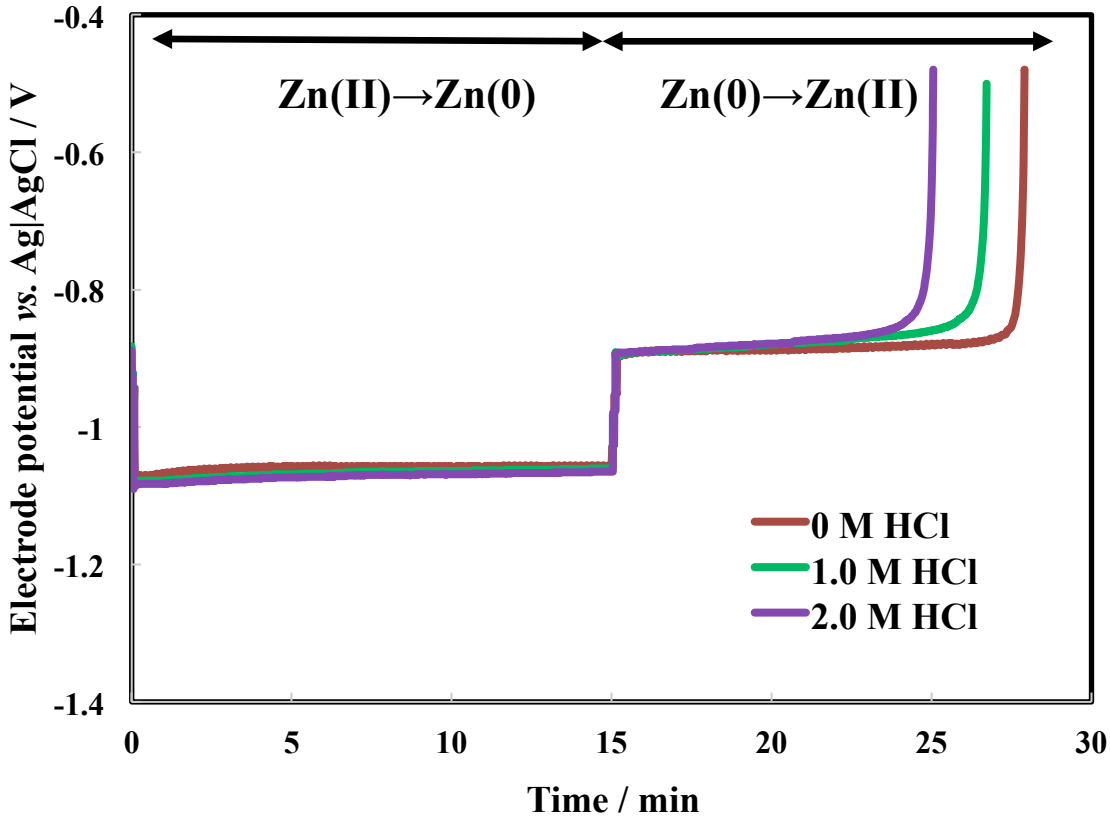


**(a)**

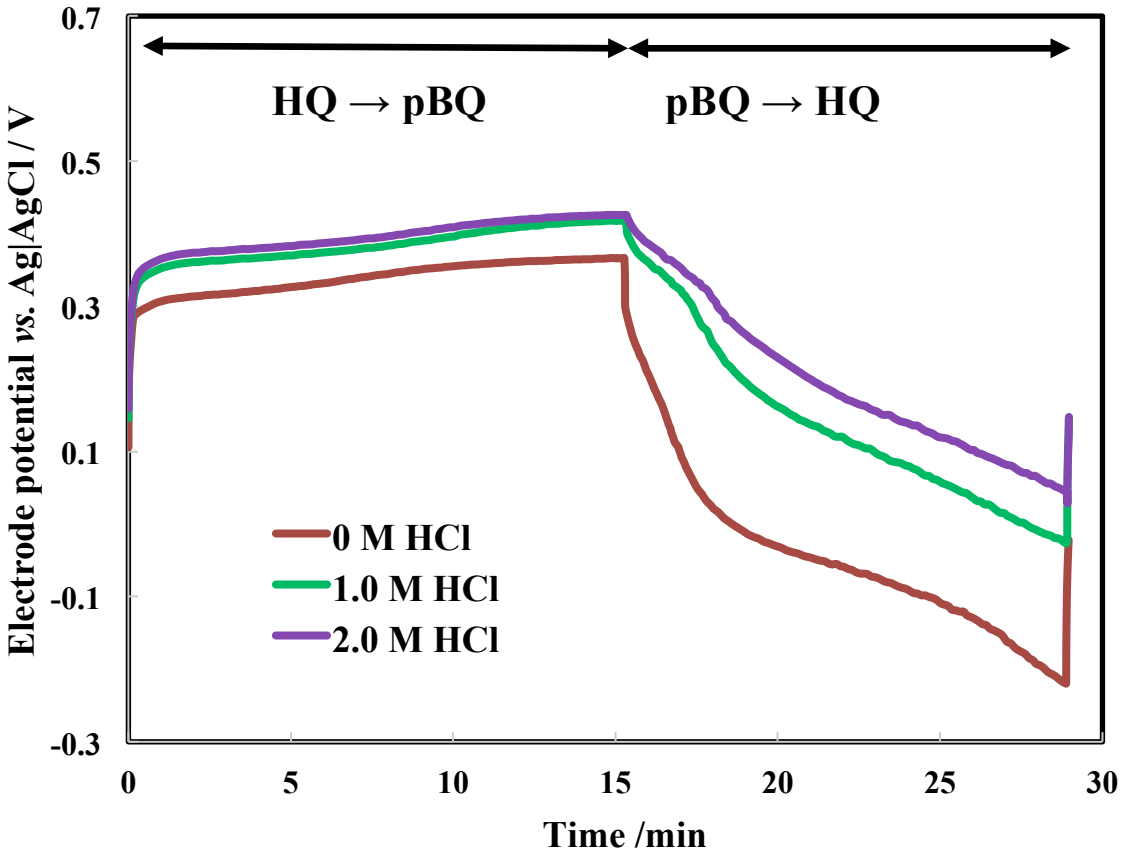


**(b)**

***Figure 5*** Effect of the hydrochloric acid concentration (0, 1 and 2 mol $dm^{-3}$) on the redox reactions of the (a) zinc and (b) parabenzoquinone (pBQ) half-cell reactions at 30 mA $cm^{-2}$. Electrolytes: 1.5 mol $dm^{-3}$ $ZnCl_2$ + 50 mmol $dm^{-3}$ hydroquinone (HQ) + HCl; working electrode for the zinc half-cell reaction: planar carbon; working electrode for the parabenzoquinone (pBQ) half-cell reaction: carbon felt; room temperature. HQ is the reduced species, pBQ is the oxidized species.

### 3.3.2. Influence of active species concentrations

In a membrane-less system, the battery reactions are highly influenced by the active species at both the negative and positive electrodes in the common electrolyte. The initial active materials were the uncharged species of zinc(II) and hydroquinone (HQ). As in Section 3.3.1., the potential measurements of the zinc negative electrode reactions were carried out by charge-discharge cycling the half-cells individually at a constant current density of 30 mA $cm^{-2}$ (120 mA) for 15 min charge and 15 min discharge in the selected pH 7 electrolytes. Figures 6a and 6b illustrate the influence of the zinc(II) species on the negative and positive electrode reactions, respectively. It can be seen that increased zinc(II) ion concentrations decreased the potential drop of the negative electrode reaction due to a more efficient transport of zinc ion from the bulk. The potential drop between charge and discharge (0.5 mol $dm^{-3}$: *c.a.* 230 mV; 1.5 mol $dm^{-3}$: *c.a.* 180 mV) of the negative electrode decreases and the half-cell coulombic efficiencies increase (0.5 mol $dm^{-3}$: *c.a.* 88 %; 1.5 mol $dm^{-3}$: *c.a.* 90 %). On the other hand, the potential drop between charge and discharge profiles of the positive electrode reaction (from *c.a.* 330 mV at 0.5 mol $dm^{-3}$ to *c.a.* 430 mV at 1.5 mol $dm^{-3}$) increases, due to the increased competition

between the active species, although the half-cell coulombic efficiency remained high at *c.a.* 93 %.

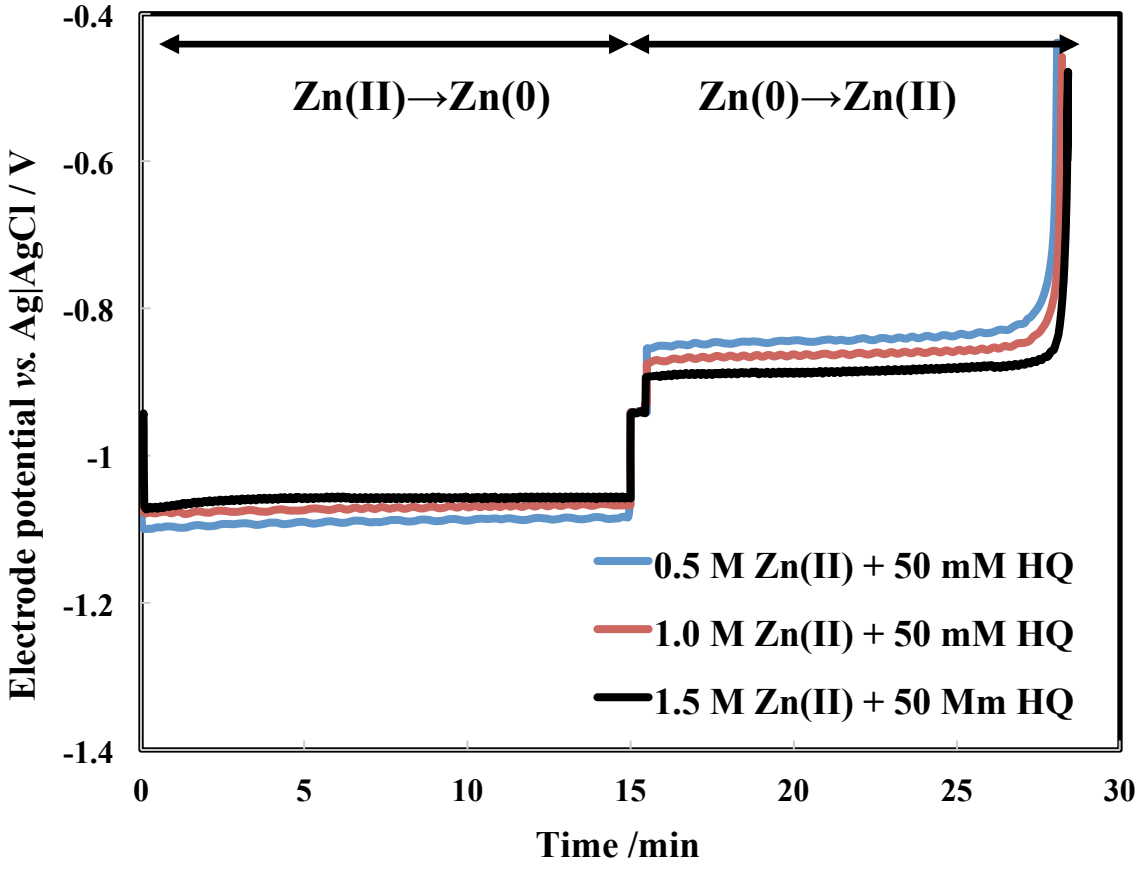


**(a)**

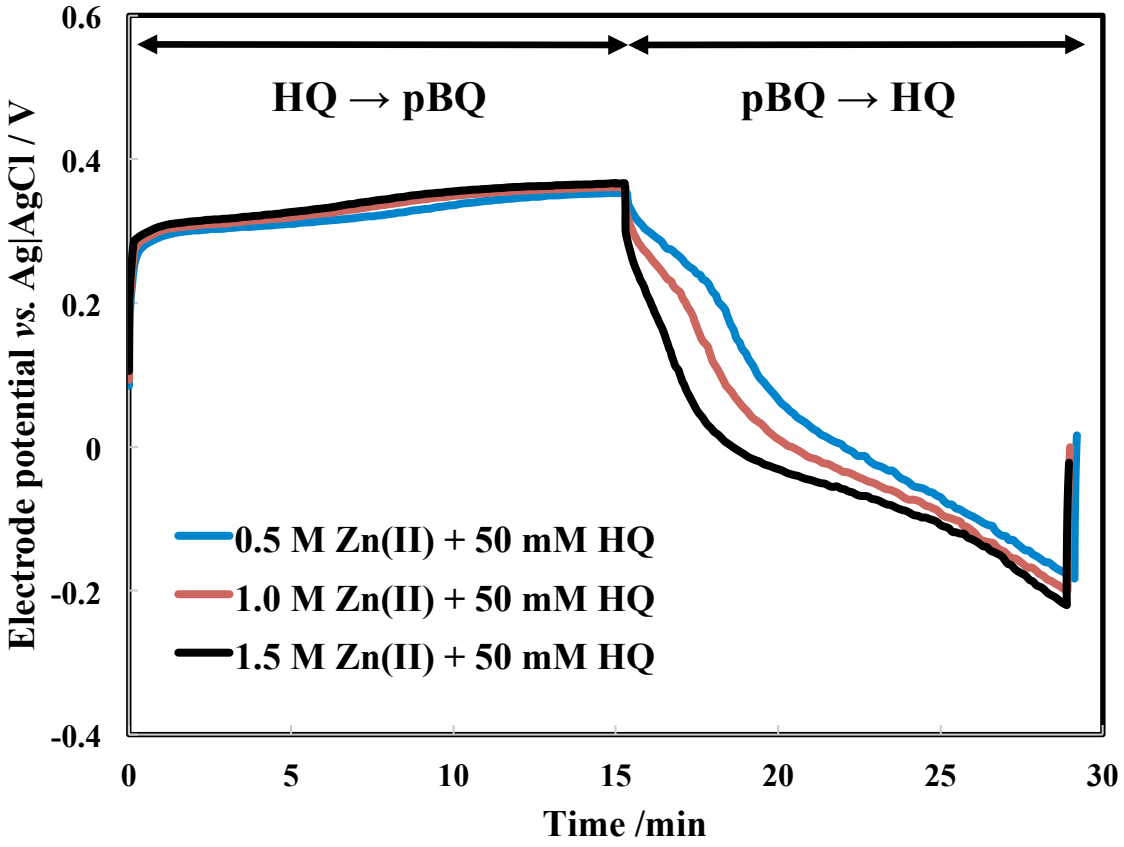


**(b)**

***Figure 6*** Effect of the zinc ion concentration (0.5, 1.0, 1.5 mol $dm^{-3}$) on the redox reactions of the (a) zinc and (b) parabenzoquinone (pBQ) half-cell reactions at 30 mA $cm^{-2}$. Electrolyte for the parabenzoquinone (pBQ) half-cell reaction: 50 mmol $dm^{-3}$ hydroquinone (HQ) + $Zn^{2+}$ (pH 7); electrode for zinc half-cell reaction: planar carbon; Electrode for parabenzoquinone (pBQ) half-cell reaction: carbon felt; room temperature. HQ is the reduced species, pBQ is the oxidized species.

Since the zinc negative electrode reaction is limiting, it is important to evaluate the influence of the oxidized and reduced quinones on the corresponding half-cell performance. Figure 7a shows the charge-discharge profile of the zinc negative electrode reaction under different concentrations of oxidized and reduced quinone (parabenzoquinone (pBQ) and hydroquinone (HQ)) species. The highest coulombic efficiency of *c.a.* 80 % was observed at a low parabenzoquinone (pBQ) concentration (10 mmol $dm^{-3}$). Since hydroquinone (HQ) and parabenzoquinone (pBQ) are the reduced and oxidized species, the compositions of these quinones track the SOC of the battery. For instance, electrolytes solely based on hydroquinone (HQ) and parabenzoquinone (pBQ) correspond to an SOC of 0 % and 100 %, respectively. With the addition of parabenzoquinone (pBQ) as the oxidizing species, the half-cell coulombic efficiency decreased significantly to *c.a.* 45 % at high concentrations (up to 90 mmol $dm^{-3}$). On the other hand, addition of the reduced hydroquinone (HQ) species did not lead to significant change in efficiency (*c.a.* 77 – 80 %,) between 10 and 90 mmol $dm^{-3}$.

The decrease in half-cell coulombic efficiencies was attributed to the competing reactions over the electrode surface as well as the self-discharge reaction between zinc and parabenzoquinone

(pBQ). In the most adverse conditions (90 mmol $dm^{-3}$ parabenzoquinone) (pBQ), the half-cell coulombic efficiency was still higher than 40 %. It should be noted that the direct chemical reactions between the metallic zinc and parabenzoquinone (pBQ) species simultaneously take place as a form of ´self-discharge´ during discharge. This is because the zinc metal is protected by the cathodic current during the charge process, when the current density is higher than the relevant corrosion current density in the system. In the case that energy needs to be stored for a long period of time, the electrolyte can be pumped out from the battery to prevent self-discharge.

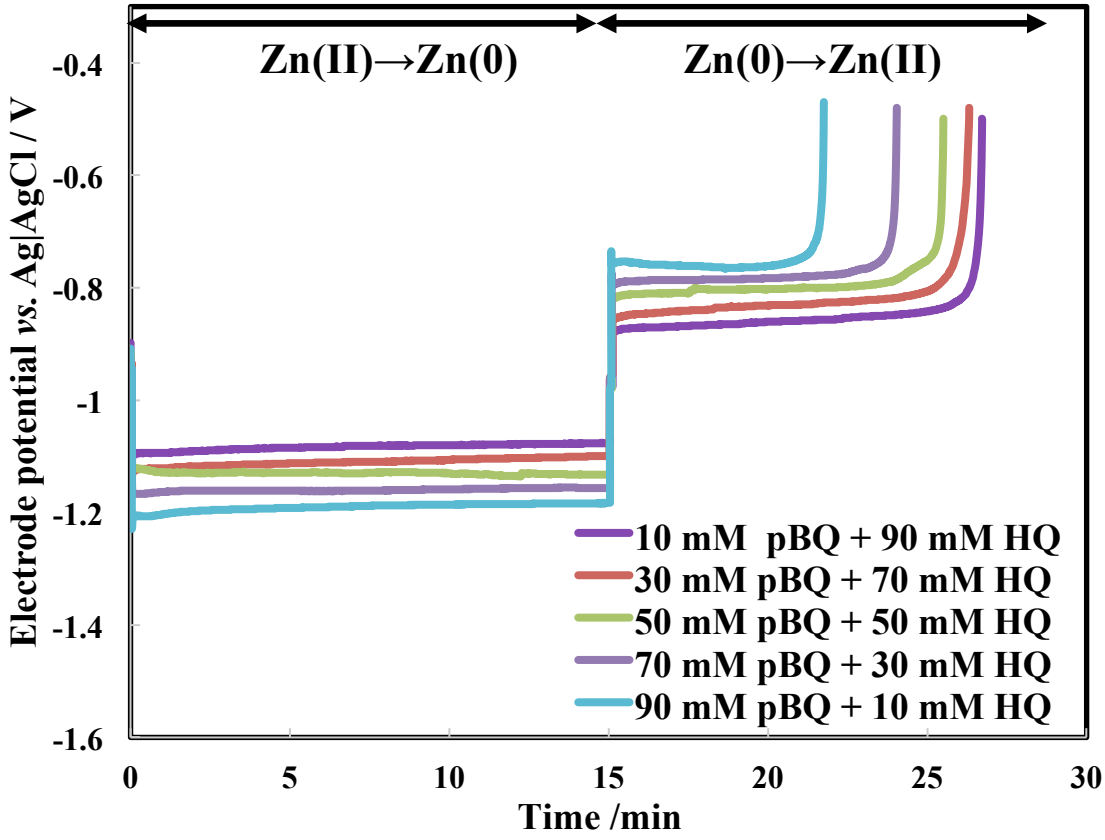


**(a)**

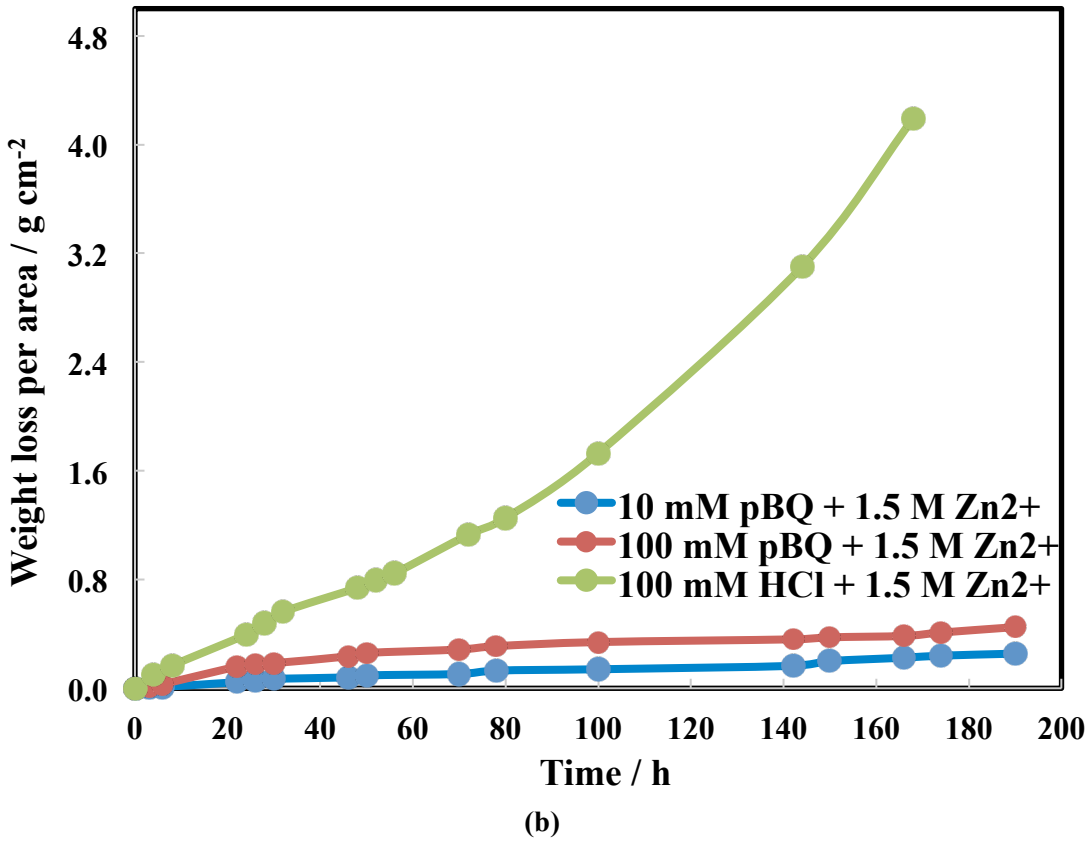


**(b)**

***Figure 7*** (a) Effect of the parabenzoquinone/ hydroquinone concentration on the redox reactions of the zinc half-cell reactions at 30 mA $cm^{-2}$. Electrolyte: 1.5 mol $dm^{-3}$ $ZnCl_2$ + parabenzoquinone (pBQ)/hydroquinone(HQ) (pH 7); electrode: planar carbon; room temperature. (b) Weight loss evolution of the metallic zinc samples under different electrolyte compositions ([parabenzoquinone] ([pBQ]), $[Zn^{2+}]$ and $[H^{+}]$) at room temperature. Electrolyte volume: 100 $cm^3$ (except 100 mmol $dm^{-3}$ HCl+ 1.5 mol $dm^{-3}$ $Zn^{2+}$, 300 $cm^3$). HQ is the reduced species, pBQ is the oxidized species.

### 3.4. Dissolution of metallic zinc

Within the membrane-less configuration, the charged products, including metallic zinc and benzoquinone, are free to react with each other as a self-discharge process. Since metallic zinc is deposited on the substrate surface, the self-discharge reactions are limited by the areas of the zinc samples exposed to the electrolytes, and can be studied by measuring the weight losses of zinc over time in the electrolytes. Figure 7b shows the dependence of the weight loss over time in different electrolyte compositions containing acid and/or parabenzoquinone (pBQ) species. It can be seen that the weight loss of zinc (up to *c.a.* 25.0 mg h $cm^{-2}$) was much more significant in the presence of acid (0.1 mol $dm^{-3}$ HCl) than in parabenzoquinone (pBQ) (at 10 and 100 mmol $dm^{-3}$). This confirms that acidic electrolytes are not suitable for zinc-based membrane-less flow batteries. At the same time, the weight loss of zinc samples was relatively slow (< 2.4 mg h $cm^{-2}$) in the presence of parabenzoquinone (pBQ) up to 100 mmol $dm^{-3}$. These losses are equivalent to corrosion current densities of < 2.0 mA $cm^{-2}$ estimated by Faraday´s law (Figure 6b). Such values are reasonably small compared to typical current densities used in redox flow battery

testing (*c.a.* 30 mA $cm^{-2}$), indicating that the proposed electrochemical reactions are suitable for a membrane-less flow battery system.

### 3.5. Galvanostatic charge-discharge cycling

Plots of the cell voltage and the half-cell electrode potentials *vs.* time of the membrane-less redox flow batteries are shown in Figure 8a. The battery was cycled at a constant current density of 30 mA $cm^{-2}$ (120 mA) under a 15 min charge – 15 min discharge regime. In most cases, the open-circuit voltages were higher than 1.05 V after the charge cycles. The average charge and discharge voltages were *c.a.* 1.51 V and *c.a.* 0.92 V, respectively. The resulting cell voltages are comparable to the membrane-based organic-inorganic systems (0.8 – 1.4 V [23, 34, 35]) and membrane-less inorganic systems (1.1 – 2.4 V [13, 14, 21, 22]).

Based on this data, the system efficiencies are summarized in Figure 9. It can be seen that the average coulombic and voltage efficiencies were *c.a.* 71.8 % and *c.a.* 58.5 %, respectively. Due to the membrane-less configuration, the coulombic effiencies obtained were lower than most batteries equipped with separators ($\eta_{col}$: > 90 % for all-vanadium and zinc-bromine batteries [3-6]). However, they are comparable to other membrane-less systems with both species dissolved in the electrolytes. For instance, the coulombic efficiencies of the soluble lead acid and zinc-cerium batteries are around 78 – 88 % at 20 – 40 mA $cm^{-2}$ as reported in the literature [13,21]. The voltage efficiencies were lower than other membrane-less systems due to the lower cell voltage and larger potential drop caused by the concentrated zinc(II) ion concentrations used to minimize the dissolution of the deposit (Figure 6b). After a number of cycles, a slight increase in the overall cell voltage was observed due to the accumulated oxidized parabenzoquinone (pBQ) species in the common electrolyte. For this reason, the zinc electrodeposit was susceptible to a faster self-discharge process, leading to a decrease in the coulombic efficiency from *c.a.* 75 % in the initial cycle down to *c.a.* 69 % after 20 cycles (Figure 8b). The fluctuations and spikes observed in latter cycles were mainly attributed to the electrolyte flow across the reference electrode, which was located at the entrance of the inlet of the flow cell as shown in Figure 2.

In all cycles, the changes in the cell voltage between the charge and discharge stages were between 600 and 735 mV. Figure 8c shows the contribution of these polarizations (half-cell overpotentials and ohmic drops) at current densities between 10 and 80 mA $cm^{-2}$. The polarizations was estimated by the overpotential, the differences between the equilibrium (open-circuit) potentials $E_{eq}$ and the electrode potentials $E$. Despite the use of a porous carbon felt electrode, the polarization of positive benzoquinone reaction (5.8 Ω $cm^2$) was even higher than that of zinc electrodeposition (2.9 Ω $cm^2$). This is attributed to the increased overpotentials caused by the competition of the active species at the electrode surface, considering that the active parabenzoquinone (pBQ) or hydroquinone (HQ) concentration (50 mmol $dm^{-3}$) is much lower than that of metallic zinc (1.5 mol $dm^{-3}$) in the common electrolytes.

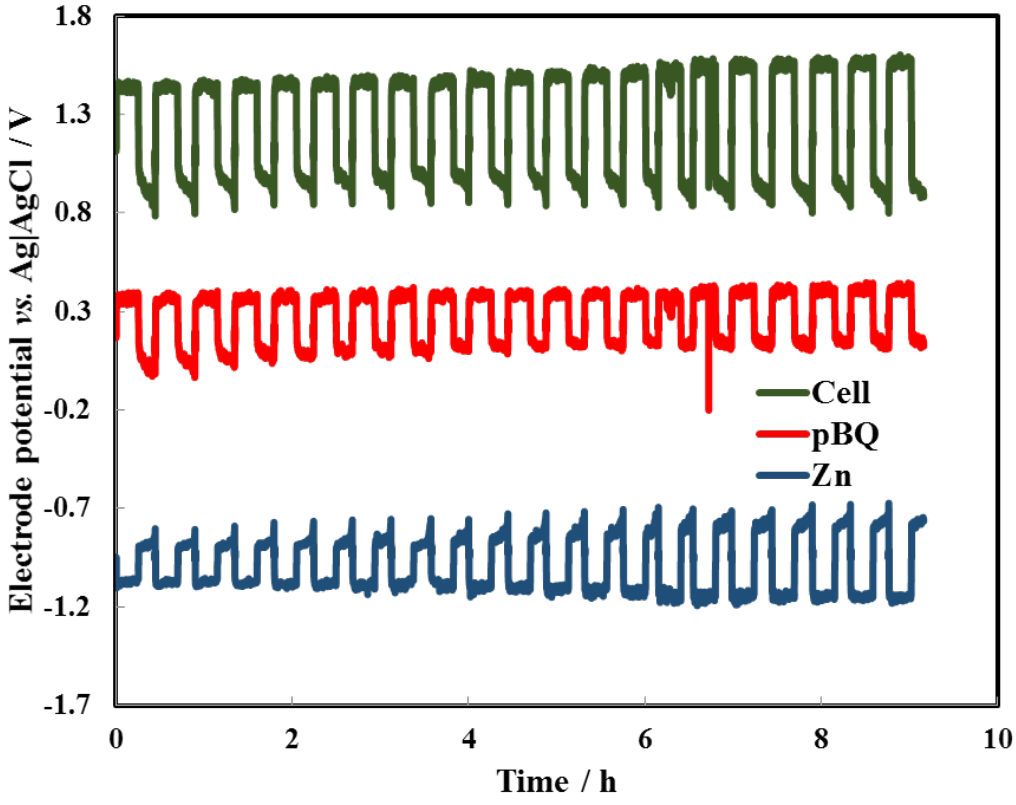
1.8
1.3
0.8
0.3
-0.2
-0.7
-1.2
-1.7
Electrode potential vs. Ag|AgCl / V
0
2
4
6
8
10
Time / h
Cell
pBQ
Zn

(a)

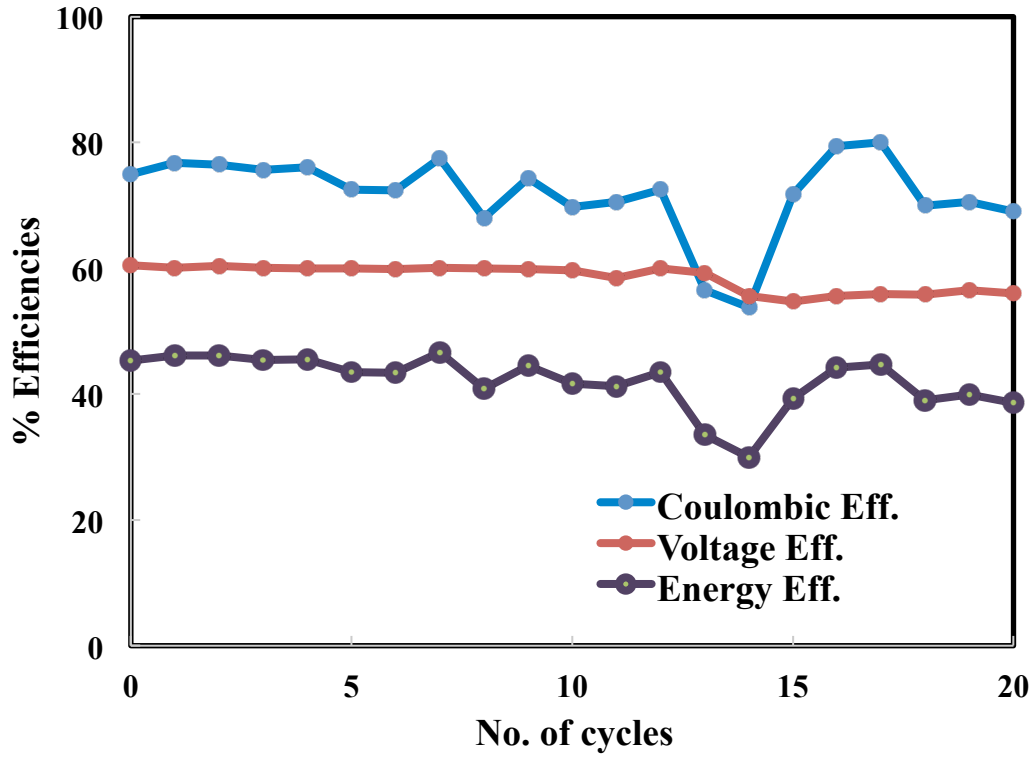
100
80
60
40
20
0
% Efficiencies
0
5
10
15
20
No. of cycles
Coulombic Eff.
Voltage Eff.
Energy Eff.

(b)

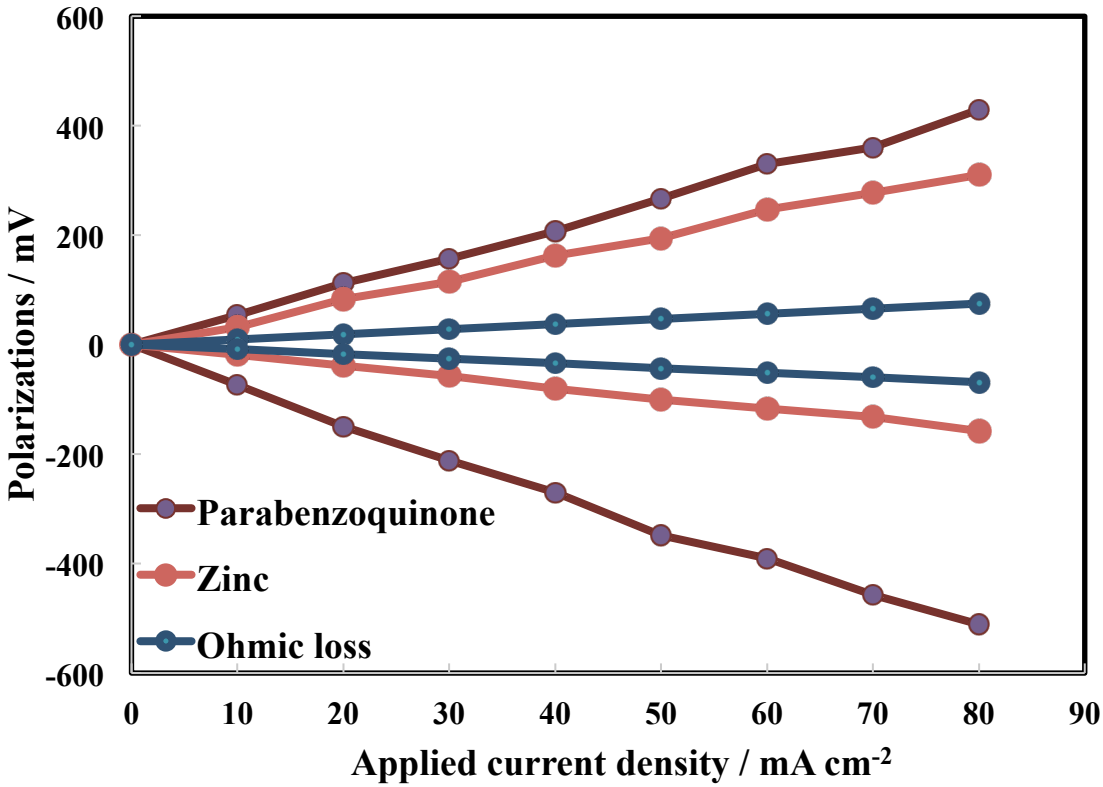


**(c)**

***Figure 8*** (a) Charge-discharge profiles of the zinc and parabenzoquinone (pBQ) electrodes as well as the overall cell voltage, (b) system efficiencies and (c) polarizations of a membraneless hybrid flow battery. Cycling conditions: 30 mA $cm^{-2}$ and room temperature. Initial electrolyte: 1.5 mol $dm^{-3}$ $ZnCl_2$ and 50 mmol $dm^{-3}$ hydroquinone (HQ); pH 7; negative electrode: planar carbon; positive electrode: carbon felt. HQ is the reduced species, pBQ is the oxidized species.

## 4. Conclusions

In this work, a membrane-less hybrid flow battery based on low-cost elements has been developed and characterised from fundamental electrochemistry to battery performance. The resulting battery has an open-circuit voltage of more than 1.05 V (after the charge cycle) and is projected to cost less than USD$ 150/ kWh. The resulting cell voltages are comparable to other membrane-based organic-inorganic systems and membrane-less inorganic systems. The concept of the battery is based on the efficiencies of the electrode reactions and the slow dissolution rate of the deposited anode in a neutral electrolyte. It was confirmed that the negative electrode reaction is limiting due to the occurrence of chemical side reactions with the positive electrode active species on the negative electrode surface.

In the presence of the oxidized parabenzoquinone species (pBQ) up to its solubility limit, the dissolution of zinc is relatively slow (< 2.37 mg $h^{-1}$ $cm^{-2}$) with an equivalent corrosion current density of < 2.0 mA $cm^{-2}$. At a current density of 30 mA $cm^{-2}$, the average coulombic and energy efficiencies of *c.a.* 71.8 and *c.a.* 42.0 %, respectively, over 20 cycles indicated stable performance. The resulting coulombic efficiencies were comparable to other membrane-less systems with both species dissolved in the electrolytes. The relatively large polarizations

observed at the positive electrode (5.8 Ω $cm^2$) were also attributed to the competition of the active species at the electrode surface, since a low concentration of quinone was used compared to the metallic zinc.

To further improve the performance in terms of higher cell voltages and efficiencies, future work should focus on the electrodeposition of zinc at higher organic species concentrations and the use of improved organic redox couples in terms of reaction kinetics, cell voltages and even solubilities, with the incorporation of functional groups (e.g., $–SO_3H$). The self-discharge of the battery should be improved with optimized electrolyte compositions and suitable corrosion inhibitors. The use of a membrane would also increase the cell voltage by permitting higher quinone concentrations. Although this would mean additional cost, the low costs of the electrolyte and active species would still lead to a relatively low overall cost of the battery.

**References**


[1] The EU Emissions Trading System (EUETS), Climate Action, http://ec.europa.eu/clima/policies/ets/index_en.htm

[2] Energy from renewable sources, Eurostat, http://ec.europa.eu/eurostat/statistics-explained/index.php/Energy_from_renewable_sources

[3] M. Skyllas-Kazacos, M.H. Chakrabarti, S.A. Hajimolana, F.S. Mjalli, M. Saleem, Progress in Flow Battery Research and Development, ***J. Electrochem. Soc.***, 2011, 158, R55-R79.

[4] J. Noack, N. Roznyatovskaya, T. Herr, P. Fischer, The Chemistry of Redox-Flow Batteries, ***Angew. Chem Int Ed.***, 2015, 54, 9776 – 9809.

[5] C. Ponce de Leon, A. Frias-Ferrer, J. Gonzalez-Garcia, D.A. Szanto, F.C. Walsh, Redox flow cells for energy conversion, ***J. Power Sources***, 2006, 160, 716 – 732.

[6] P. Leung, X. Li, C. Ponce de Leon, L. Berlouis, C.T.J. Low, F.C. Walsh, Progress in redox flow batteries, remaining challenges and their applications in energy storage, ***RSC Adv.***, 2012, 2, 10125-10156.

[7] Grid Energy Storage, U.S. Department of Energy, 2013.

http://energy.gov/oe/downloads/grid-energy-storage-december-2013

[8] M.R. Mohamed, P.K. Leung, M.H. Sulaiman, Performance characterization of a vanadium redox flow battery at different operating parameters under a standardized test-bed system, ***Applied Energy***, 2015, 137, 402-412.

[9] P.K. Leung, C. Ponce de Leon, C.T.J. Low, A.A. Shah, F.C. Walsh, Characterization of a zinc-cerium flow battery, ***J. Power Sources***, 2011, 196, 5174 – 5185.

[10] P.K. Leung, M.R. Mohamed, A.A. Shah, Q. Xu, M. B. Conde-Duran, A mixed acid based vanadium-cerium redox flow battery with a zero-gap serpentine architecture***, J. Power Sources***, 2015, 274, 651 – 658

[11] S. Eckroad, 'Vanadium redox flow batteries: An in-depth analysis'. (Technical Report EPRI-1014836, Electric Power Research Institute, Palo Alto, CA, 2007.

http://www.paredox.com/foswiki/pub/Trash/TrashAttachment/EPRI_-_Vanadium_Redox_Flow_Batteries_2007_.pdf

[12] Y.K. Zeng, T.S. Zhao, L. An, X.L. Zhou, L. Wei, A comparative study of all-vanadium and iron-chromium redox flow batteries for large-scale energy storage, J. Power Sources, 2015, 300, 438 – 443.

[13] D. Pletcher, R. Wills, A novel flow battery: A lead acid battery based on an electrolyte with soluble lead(II). Part II. Flow cell studies, ***Phys. Chem. Chem. Phys.***, 2004, 6, 1779 – 1785.

[14] R. G. A. Wills, J. Collins, D. Stratton-Campbell, C.T.J. Low, D. Pletcher, F.C. Walsh, Developments in the soluble lead-acid flow battery, ***J. Appl. Electrochem.***, 2010, 40, 955 – 965.

[15] J. Cheng, L. Zhang, Y-S. Yang, Y-H. Wen, G-P. Cao, X-D. Wang, Preliminary study of single flow zinc-nickel battery, ***Electrochem. Communications***, 2007, 9, 2639 – 2642.

[16] Y. Cheng, H. Zhang, Q. Lai, X. Li, D. Shi, L. Zhang, A High power density single flow zinc-nickel battery with three-dimensional porous negative electrode, ***J. Power Sources***, 2013, 241, 196 – 202.

[17] J. Pan, Y. Sun, J. Cheng, Y. Wen, Y. Yang, P. Wan, Study on a new single flow acid Cu-$PbO_2$ battery, ***Electrochem. Communications,*** 2008, 10, 1226 – 1229.

[18] Y. Xu, Y. Wen, J. Cheng, G.G.Y. Yang, Study on a single flow acid Cd-chloranil battery, ***Electrochem. Communications,*** **11** (2009) 1422 - 1424.

[19] P.K. Leung, Q. Xu, T.S. Zhao, High-potential zinc-lead dioxide rechargeable cells, ***Electrochim. Acta***, 2012, 79, 117 – 125.

[20] J. Pan, Y. Wen, J. Cheng, J. Pan, S. Bai, Y. Yang, Evolution of substrates of zinc negative electrode in acid $PbO_2$-Zn single flow batteries, ***Chinese Journal of Chemical Engineering***, 2016, 24, 529 – 534.

[21] P.K. Leung, C. Ponce de Leon, F.C. Walsh, An undivided zinc-cerium redox flow battery operating at room temperature (295 K), ***Electrochem. Communications,*** 2011, 13, 770 – 773.

[22] P.K. Leung, C. Ponce de Leon, F.C. Walsh, The influence of operational parameters on the performance of an undivided zinc-cerium flow battery, ***Electrochim. Acta***, 2012, 80, 7 – 14.

[23] B. Huskinson, M.P. Marshak, C.W. Suh, S. Er, M.R. Gerhardt, C.J. Galvin, X.D. Chen, A. Aspuru-Guzik, R.G. Gordon, M.J. Aziz, 'A metal-free organic-inorganic aqueous flow battery', ***Nature***, 505 (2014) 195 – 198

[24] R.M. Darling, K.G. Gallagher, J.A. Kowalski, S. Ha, F.R. Brushett, 'Pathways to low-cost electrochemical energy storage: a comparison of aqueous and nonaqueous flow batteries', ***Energy Environ. Sci***., 7 (2014) 3459 - 3477.

[25] T.B. Schon, B.T. McAllister, P.-F. Li, D.S. Seferos, 'The rise of organic electrode materials for energy storage', ***Chem. Soc. Rev***., (2016) accepted

[26] L. Cheng, R.S. Assary, X.H. Qu, A. Jain, S.P. Ong, N.N. Rajput, K. Persson, L.A. Curtiss, 'Accelerating Electrolyte Discovery for Energy Storage with High-Throughput Screening', ***J. Phys. Chem. Lett.***, 6 (2015) 283−291

[27] S.D. Pineda Flores, G.C. Martin-Noble, R.L. Phillips, J. Schrier, 'Bio-Inspired Electroactive Organic Molecules for Aqueous Redox Flow Batteries. 1. Thiophenoquinones', ***J. Phys. Chem. C.***, 119 (2015) 21800 – 21809

[28] Y. Moon, Y.K. Han, 'Computational screening of organic molecules as redox active species in redox flow batteries', ***Current Applied Physics***, 1 (2016) 939 – 943

[29] T. Janoschka, N. Martin, U. Martin, C. Friebe, S. Morgenstern, H. Hiller, M.D. Hager, U.S. Schubert, 'An aqueous, polymer-based redox-flow battery using non-corrosive, safe, and low-cost materials', ***Nature***, 527 (2015) 78 – 81

[30] Y. Xu, Y. Wen, J. Cheng, G.G.Y. Yang, 'Study on a single flow acid Cd-chloranil battery', ***Electrochemistry Communications***, 11 (2009) 1422 – 1424.

[31] K. Gong, Q. Fang, S. Gu, S. F. Y. Li, Y. Yan, Nonaqueous Redox-Flow Batteries: Organic Solvents, Supporting Electrolytes, and Redox Pairs, *Energy Environ.* ***Sci.***, 2015, 8, 3515 – 3530.

[32] Alibaba.com,

http://www.alibaba.com/trade/search?fsb=y&IndexArea=product_en&CatId=&SearchText=Propylene+carbonate

[33] European Environmental Agency, Agricultural, Industrial and Household water prices in late 1990s,

http://www.eea.europa.eu/data-and-maps/figures/agricultural-industrial-and-household-water-prices-in-late-1990s

[34] K. Lin, R. Gomez-Bombarelli, E.S. Beh, L. Tong, Q. Chen, A. Valle, A. Aspuru-Guzik, M.J. Aziz, R.G. Gordon, A redox- flow battery with an alloxazine-based organic electrolyte, ***Nature Energy***, 2016, 1, 16102.

[35] K. Lin, Q. Chen, M.R. Gerhardt, L. Tong, S. B. Kim, L. Eisenach, A. W. Valle, D. Hardee, R.G. Gordon, M.J. Aziz, M. P. Marshak, Alkaline quinone flow battery, ***Science***, 2015, 349, 1529 – 1532.

[36] B. Yang, L. Hoober-Burkhardt, F. Wang, G.K. Surya Prakash, S.R. Narayanan, An Inexpensive Aqueous Flow Battery for Large-Scale Electrical Energy Storage Based on Water-Soluble Organic Redox Couples, ***J. Electrochem. Soc.***, 2014, 161, A1371– A1380.

[37] S. Er, C. Suh, M.P. Marshak, A. Aspuru-Guzik, Computational design of molecules for an all-quinone redox flow battery, ***Chem. Sci.***, 2015, 6, 885 – 893.

[38] Stuart I. Bailey, Ian M. Ritchie, The Construction and Use of Potential-pH Diagrams in Organic Oxidation-Reduction Reactions, ***J. Chem. Soc. Perkin Trans***, 11, 1983, 645.

[39] W. A. Furtado, L. D. Dos Santos, An Alkaline Electrolytic Bath and a process for electrodeposition of Cu, Zn, OR Ni, As Well As Their Alloys, ***WO Patent 1998018982 A1***, 7th May, 1887.

[40] P.K. Leung, C. Ponce de Leon, F.J. Recio, P. Herrasti, F.C. Walsh, Corrosion of the zinc negative electrode of zinc-cerium hybrid redox flow batteries in methanesulfonic acid, ***J. Appl. Electrochem***., 2014, 44, 1025 – 1035.

[41] B. Kavitha, P. Santhosh, M. Renukadevi, A. Kalpana, P. Shakkthivel, T. Vasudevan, Role of Organic Additives on Zinc Plating, ***Surface & Coating Techn.***, 2006, 201, 3438 – 3442.

[42] P. Leung, J. Palma, E. Garcia-Quismondo, L. Sanz, M.R. Mohamed, M. Anderson, Evaluation of electrode materials for all-copper hybrid flow batteries, ***J. Power Sources***, 2016, 310, 1 – 11.

[43] M. Quan, D. Sanchez, M.F. Wasylkiw, D.K. Smith, 'Voltammetry of Quinones in Unbuffered Aqueous Solution: Reassessing the Roles of Proton Transfer and Hydrogen Bonding in the Aqueous Electrochemistry of Quinones', ***J. Am. Soc.,*** 2007, 129, 12847 - 12856.

[44] Q. Lai, H. Zhang, X. Li, L. Zhang, Y. Cheng, A novel single flow zinc-bromine battery with improved energy density, *J. Power Sources*, 2013, 235, 1 – 4.

[45] H. S. Yang, J. H. Park, H. W. Ra, C-S. Jin, J.H. Yang, Critical rate of electrolyte circulation for preventing zinc dendrite in a zinc-bromine redox flow battery, *J. Power Sources*, 2016, 325, 446 – 452.

# Electronic Supplementary Information

## Membrane-less hybrid flow battery based on low-cost elements

P.K. Leung[1,2], T. Martin[1], A.A. Shah[3,†] , M.R. Mohamed[4], M.A. Anderson[1], J. Palma[1]

1. IMDEA Energy, Mostoles, Madrid, 28935, Spain.

2. Department of Materials, University of Oxford, Oxford, OX1 3PH, UK.

3. School of Engineering, University of Warwick, Coventry, CV4 7AL, UK.

4. Faculty of Electrical & Electronics, Universiti Malaysis Pahang, 26600, Malaysia.

**Component costs of redox flow battery module:**

| Components | Cost | References |
|---|---|---|
| Bipolar plate, USD$ $m^{-2}$ | 55 | [S1] |
| Graphite felt, USD$ $m^{-2}$ | 70 | [S1] |
| PVC frame, USD$ $m^{-2}$ | 16.56 | [S1] |
| Membrane, USD$ $m^{-2}$ | 500 | [S1] |
| Gakets, bolts, end-plate, USD$ $m^{-2}$ | 14 | [S1] |
| Heat exchanger, USD$ $kW^{-1}$ | 84 | [S1] |
| Thermal insulation material, USD$ $m^{-2}$ | 15 | [S1] |
| Electrolyte tank, USD$ $gallon^{-1}$ | 0.29 | [S1] |
| Rebalance cell, USD$ $kW^{-1}$ | 8.27 | [S1] |
| Pump, per item, USD$ (2 pumps per stack) | 178 | [S2] |
| Battery management system, per item, USD$ (1 battery management system per stack) | 550 | [S2] |
| Vanadium, USD$ $kg^{-1}$ | 23.6 | [S3] |
| Zinc, USD$ $kg^{-1}$ | 2.3 | [S3] |
| Para-benzoquinone (pBQ), USD$ $kg^{-1}$ | 5 | [S4] |

**Calculation of electrolyte costs based on active materials**

| Elements | Cost | Molecular weight | Capacity in 1 Kg |
|---|---|---|---|
| Vanadium | USD$23.6 $Kg^{-1}$ | 50.94 g $mol^{-1}$ | 526 Ah (1 $e^-$) |
| Zinc | USD$2.3 $Kg^{-1}$ | 65.38 g $mol^{-1}$ | 820 Ah (2 $e^-$) |
| Parabenzoquinone (pBQ) | USD$5 $Kg^{-1}$ | 108.1 g $mol^{-1}$ | 496 Ah (2 $e^-$) |

†Corresponding author. *Tel*: +44 (0)2476 151676. *Fax*: +44 (0)2476 418922. *Email*: Akeel.Shah@warwick.ac.uk

**Electrolyte cost based on active materials per 1 kWh**

| Chemistry | Energy | Discharge voltage | Required capacity | Weight of active materials | Cost of active materials |
|---|---|---|---|---|---|
| All-vanadium | 1000 Wh | 1.30 V | 769 Ah | 1.46 kg V + 1.46 kg V | $ 68.9 |
| Zinc-para-benzoquinone (pBQ) | 1000 Wh | 0.92 V | 1086 Ah | 1.33 kg Zn + 2.18 kg pBQ | $ 14.0 |

**Specification of a 1 MW × 10 h systems in the cost model**

| | All-vanadium | Zinc-para-benzoquinone (pBQ) |
|---|---|---|
| **System power output** | 1 MW × 10 h | 1 MW × 10 h |
| **Discharge cell voltage** | 1.3 V (single cell) | 0.92 V (single cell) |
| **Current density** | 50 mA $cm^{-2}$ (single cell) | 30 mA $cm^{-2}$ (single cell) |
| **Coulombic efficiency** | 95 % (single cell & whole system) | 72 % (single cell & whole system) |
| **Power of system loss** | 40 kW [S1] | 40 kW [S1] |

**Dimensions of a 100-cells stack based on Regenesys® module**

**Dimension of each 100-cells stack:** 155 cm × 150 cm × 80 cm **(see Figure S1a)**

**Inter-electrode gap:** 0.75 cm **(see Figure S1b)**

**Electrode area:** 108 cm × 67 cm = 7236 $cm^2$ or 0.723 $m^2$ **(see Figure S1c)**

**PVC frame area:** 108 cm × 67 cm = 7236 $cm^2$ or 0.723 $m^2$ **(see Figure S1c)**

**Membrane area (assumed):** 110 cm × 70 cm = 7700 $cm^2$ or 0.77 $m^2$ **(see Figure S1c)**

**Dimension of electrolyte tank:** 2 m diameter

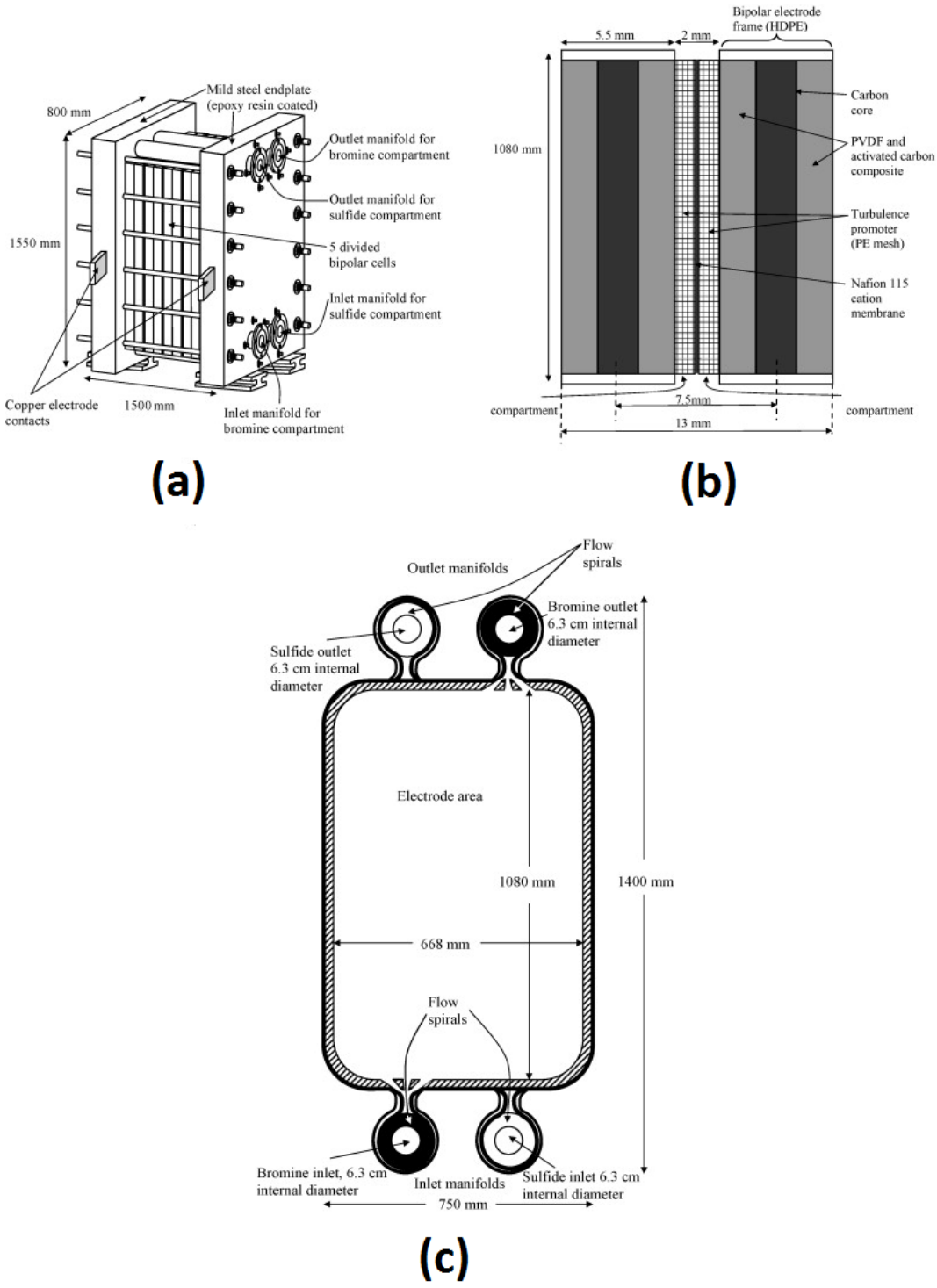


Figure S1. (a) Lateral view of the Regenesys® module showing the inlet and outlet manifolds and the location of the current collectors. Not to scale. (b) Details of a bipolar cell showing the main components. Not to scale. The dimensions are nominal. (c) Electrode configuration showing the location of the spirals and the projected electrode area [S5].

**Power output for each Regenesys® module using all-vanadium chemistry**

= Current × (Voltage × 100 cells) × Time × Coloumbic Eff.

= (7236 $cm^2$ × 0.05 A $cm^{-2}$) × (1.3 V × 100 cells) × 10 h × 95 %

= 446823 Wh or 446.8 kWh

**Power output for each Regenesys® module using zinc-parabenzoquinone (pBQ) chemistry**

= Current × (Voltage × 100 cells) × Time × Coloumbic Eff.

= (7236 $cm^2$ × 0.03 A $cm^{-2}$) × (0.92 V × 100 cells) × 10 h × 72 %

= 143793 Wh or 143.8 kWh

**Number of Regenesys® module required for a 1 MW × 10 h system**

Power requirement (including 40 kW system loss):

= (1000 + 40) kW × 10 h

= 10400 kWh

Number of Regenesys® module required for all-vanadium chemistry:

= 10400 kWh ÷ 446.8 kWh per module

= 23.3 Regenesys® modules

Number of Regenesys® module required for zinc-parabenzoquinone (pBQ) chemistry:

= 10400 kWh ÷ 143.8 kWh per module

= 72.3 Regenesys® modules

**Mass of active materials required for a 1 MW × 10 h system**

For all-vanadium chemistry:

= 15185 kg vanadium (negative) + 15185 kg vanadium (positive)

= 30370 kg

For zinc-parabenzoquinone (pBQ) chemistry:

= 13832 kg zinc (negative) + 22672 kg parabenzoquinone (pBQ) (positive)

**Volume of electrolytes required for a 1 MW × 10 h system**

For all-vanadium chemistry:

= 199802.5 L of 1.5 M vanadium solution × 2

= 388605 L of 1.5 M vanadium solution (negative & positive electrolytes) (102659 gallons)

For zinc-parabenzoquinone (pBQ) chemistry:

= 2099305 L of 0.1 M hydroquinone (HQ)/ zinc(II) solution (single electrolyte) (554578 gallons)

**Estimated cost of a 1 MW × 10 h system using all-vanadium chemistry**

**(a) Cost of bipolar plate**

= 0.723 $m^2$ × 101 items ×USD$ 55 $m^{-2}$ × 23.3 stacks

= USD$ 93579

**(b) Cost of graphite felts**

= 0.723 $m^2$ × 200 items ×USD$ 70 $m^{-2}$ × 23.3 stacks

= USD$ 235842

**(c) Cost of PVC frame**

= 0.723 $m^2$ × 101 items ×USD$ 16.6 $m^{-2}$ × 23.3 stacks

= USD$ 28243

**(d) Cost of membrane**

= 0.77 $m^2$ × 100 items ×USD$ 500 $m^{-2}$ × 23.3 stacks

= USD$ 897050

**(e) Cost of gaskets, bolts and end-plates**

= 0.723 $m^2$ × 200 items ×USD$ 14 $m^{-2}$ × 23.3 stacks

= USD$ 47169

**(f) Cost of heat exchanger**

= 1040 kW ×USD$ 84 $kW^{-1}$

= USD$ 87360

**(g) Cost of thermal insulation material**

= Area surrounding the tank ×USD$ 15 $m^{-2}$

= 790 $m^2$ ×USD$ 15 $m^{-2}$

= USD$ 63360

**(h) Cost of electrolyte tanks**

= 102659 gallons × USD$ 0.29 $gallon^{-1}$

= USD$ 29771

**(i) Cost of pumps**

= 2 items × USD$ 178 × 23.3 stacks

= USD$ 8295

**(j) Cost of battery management systems**

= 1 item × USD$ 550 × 23.3 stacks

= USD$ 12815

**(k) Cost of rebalance cell**

= USD$ 8.27 $kW^{-1}$ × 1040 kW

= USD$ 8600

**(l) Cost of electrolytes (based on active materials)**

= 30370 kg vanadium × USD$ 23.6 $kg^{-1}$

= USD$ 716732

**Total Cost for all-vanadium chemistry:**

| Cell components | Cost / USD$ | Cost per kWh / USD$ $kWh^{-1}$ | Percentage / % |
|---|---|---|---|
| Bipolar plate | 93579 | 9.4 | 4.3 |
| Carbon felt | 235842 | 23.6 | 10.8 |
| PVC frame | 28243 | 2.8 | 1.3 |
| Membrane | 897050 | 89.7 | 41.2 |
| Gaskets, bolts, etc | 47169 | 4.7 | 2.2 |
| Heat exchanger | 87360 | 8.7 | 4.0 |
| Thermal insulation material | 11850 | 1.2 | 0.5 |
| Tanks | 29771 | 3.0 | 1.4 |
| Pumps | 8295 | 0.8 | 0.4 |
| Battery management | 12815 | 1.3 | 0.6 |
| Rebalance cell | 8600 | 0.9 | 0.4 |
| Electrolytes | 716732 | 71.7 | 32.9 |
| **Total** | **2177306** | **217.7** | **100** |

**Estimated cost of a 1 MW × 10 h system using zinc-para-benzoquinone** (pBQ) **chemistry**

**(a) Cost of bipolar plate**

= 0.723 $m^2$ × 101 items ×USD$ 55 $m^{-2}$ × 72.3 stacks

= USD$ 290376

**(b) Cost of graphite felts**

= 0.723 $m^2$ × 100 items ×USD$ 70 $m^{-2}$ × 72.3 stacks

= USD$ 365910

**(c) Cost of PVC frame**

= 0.723 $m^2$ × 101 items ×USD$ 16.6 $m^{-2}$ × 72.3 stacks

= USD$ 87641

**(d) Cost of membrane**

= 0.77 $m^2$ × 0 items ×USD$ 500 $m^{-2}$ × 72.3 stacks

= USD$ 0

**(e) Cost of gaskets, bolts and end-plates**

= 0.723 $m^2$ × 200 items ×USD$ 14 $m^{-2}$ × 72.3 stacks

= USD$ 146364

**(f) Cost of heat exchanger**

= 1040 kW ×USD$ 84 $kW^{-1}$

= USD$ 87360

**(g) Cost of thermal insulation material**

= Area surrounding the tank ×USD$ 15 $m^{-2}$

= 4211 $m^2$ ×USD$ 15 $m^{-2}$

= USD$ 63165

**(h) Cost of electrolyte tanks**

= 554578 gallons × USD$ 0.29 $gallon^{-1}$

= USD$ 160828

**(i) Cost of pumps**

= 2 items × USD$ 178 × 72.3 stacks

= USD$ 25738

**(j) Cost of battery management systems**

= 1 item × USD$ 550 × 23.3 stacks

= USD$ 39765

**(k) Cost of rebalance cell**

**=** USD$ 8.27 $kW^{-1}$ × 1040 kW

= USD$ 8600

**(l) Cost of electrolytes (based on active materials)**

= 13832 kg zinc × USD$ 2.3 $kg^{-1}$ + 22672 kg parabenzoquinone (pBQ) × USD$ 5.0 $kg^{-1}$

= USD$ 145174

| **Cell components** | **Cost / USD$** | **Cost per kWh / USD$ $kWh^{-1}$** | **Percentage / %** |
|---|---|---|---|
| Bipolar plate | 290376 | 29.0 | 20.4 |
| Carbon felt | 365910 | 36.6 | 25.8 |
| PVC frame | 87641 | 8.8 | 6.2 |
| Membrane | 0 | 0 | 0 |
| Gaskets, bolts, etc | 146364 | 14.6 | 10.3 |
| Heat exchanger | 87360 | 8.7 | 6.2 |
| Thermal insulation material | 63165 | 6.3 | 4.4 |
| Tanks | 160828 | 16.1 | 11.3 |
| Pumps | 25738 | 2.6 | 1.8 |
| Battery management | 39765 | 4.0 | 2.8 |
| Rebalance cell | 8600 | 0.9 | 0.6 |
| Electrolytes | 145174 | 14.5 | 10.2 |
| **Total** | **1420921** | **142.1** | **100** |

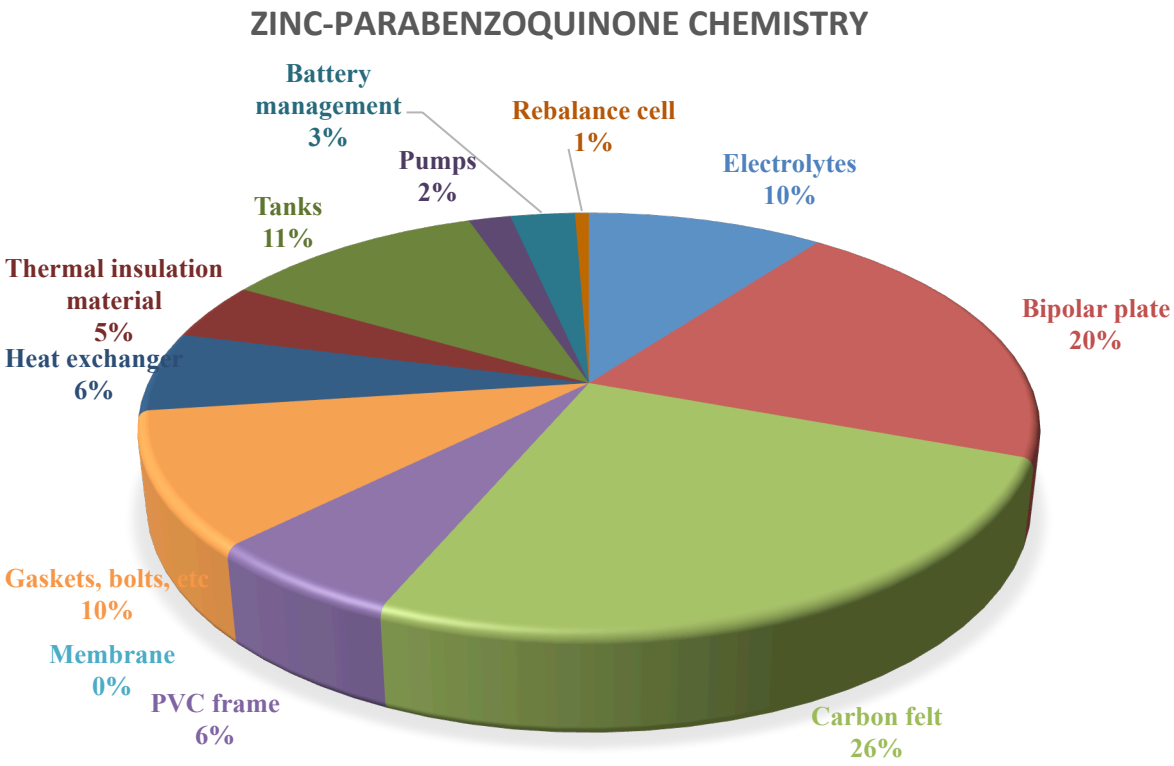


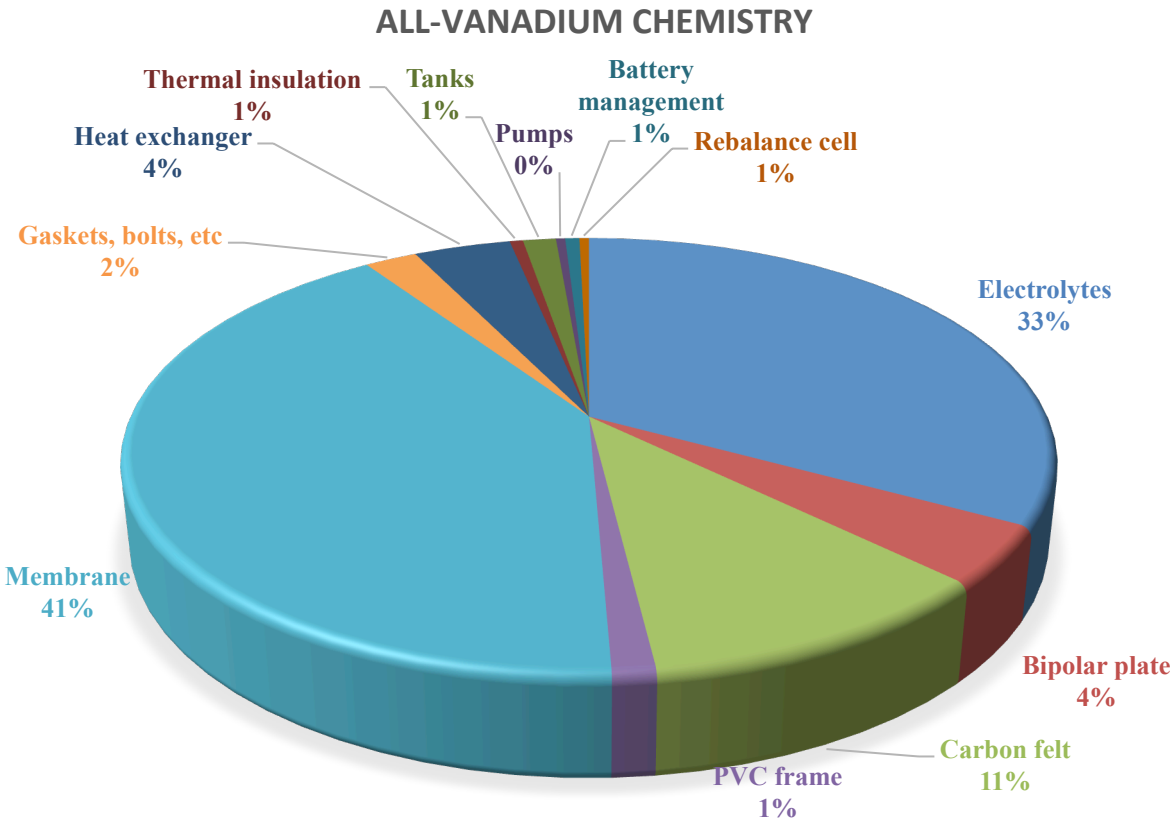


**Cost comparisons of zinc-parabenzoquinone (pBQ) and all-vanadium systems (1 MW × 10 h)**

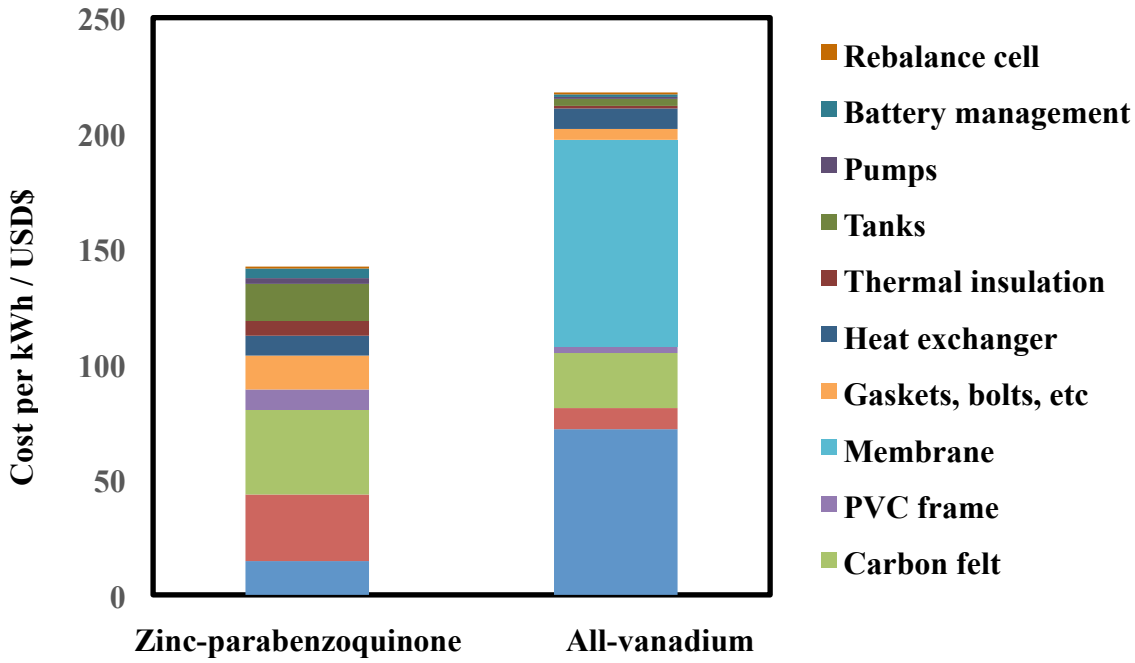


**References**


[S1] Y.K. Zeng, T.S. Zhao, L. An, X.L. Zhou, L. Wei, A comparative study of all-vanadium and iron-chromium redox flow batteries for large-scale energy storage, J. Power Sources, 2015, 300, 438 – 443.

[S2] L. Joerissen, J. Garche, Ch. Fabjan, G. Tomazic, Possible use of vanadium redox-flow batteries for energy storage in small grids and stand-alone photovoltaic systems, *J. Power Sources*, 127, 2004, 98 -104.

[S3] http://mineralprices.com/

[S4] https://www.alibaba.com/product-detail/HQ-hydroquinone-price_60378721262.html?spm=a2700.7724838.0.0.TqxgTg&s=p

[S5] C. Ponce de Leon, G.W. Reade, I. Whyte, S.E. Male, F.C. Walsh, Characterization of the reaction environment in a filter-press redox flow reactor, Electrochim. Acta, 2007, 52, 5815 – 5823.